

UNCLASSIFIED

AD NUMBER
ADB265599
NEW LIMITATION CHANGE
TO Approved for public release, distribution unlimited
FROM Distribution authorized to U.S. Gov't. agencies only; Proprietary Info.; Jun 2001. Other requests shall be referred to US Army Medical Research and Materiel Comd., 504 Scott St., Fort Detrick, MD 21702-5012.
AUTHORITY
USAMRMC ltr, dtd 21 Feb 2003

THIS PAGE IS UNCLASSIFIED

AD _____

Award Number: DAMD17-97-1-7207

TITLE: Template Based Design of Anti-Metastatic Drugs from the
Active Conformation of Laminin Peptide II

PRINCIPAL INVESTIGATOR: Jean R. Starkey, Ph.D.

CONTRACTING ORGANIZATION: Montana State University
Bozeman, Montana 59717-2470

REPORT DATE: January 2001

TYPE OF REPORT: Annual

PREPARED FOR: U.S. Army Medical Research and Materiel Command
Fort Detrick, Maryland 21702-5012

DISTRIBUTION STATEMENT: Distribution authorized to U.S. Government
agencies only (proprietary information, Jan 01). Other requests
for this document shall be referred to U.S. Army Medical Research
and Materiel Command, 504 Scott Street, Fort Detrick, Maryland
21702-5012.

The views, opinions and/or findings contained in this report are
those of the author(s) and should not be construed as an official
Department of the Army position, policy or decision unless so
designated by other documentation.

20010430 031

NOTICE

USING GOVERNMENT DRAWINGS, SPECIFICATIONS, OR OTHER DATA INCLUDED IN THIS DOCUMENT FOR ANY PURPOSE OTHER THAN GOVERNMENT PROCUREMENT DOES NOT IN ANY WAY OBLIGATE THE U.S. GOVERNMENT. THE FACT THAT THE GOVERNMENT FORMULATED OR SUPPLIED THE DRAWINGS, SPECIFICATIONS, OR OTHER DATA DOES NOT LICENSE THE HOLDER OR ANY OTHER PERSON OR CORPORATION; OR CONVEY ANY RIGHTS OR PERMISSION TO MANUFACTURE, USE, OR SELL ANY PATENTED INVENTION THAT MAY RELATE TO THEM.

LIMITED RIGHTS LEGEND

Award Number: DAMD17-97-1-7207

Organization: Montana State University

Location of Limited Rights Data (Pages):

Those portions of the technical data contained in this report marked as limited rights data shall not, without the written permission of the above contractor, be (a) released or disclosed outside the government, (b) used by the Government for manufacture or, in the case of computer software documentation, for preparing the same or similar computer software, or (c) used by a party other than the Government, except that the Government may release or disclose technical data to persons outside the Government, or permit the use of technical data by such persons, if (i) such release, disclosure, or use is necessary for emergency repair or overhaul or (ii) is a release or disclosure of technical data (other than detailed manufacturing or process data) to, or use of such data by, a foreign government that is in the interest of the Government and is required for evaluational or informational purposes, provided in either case that such release, disclosure or use is made subject to a prohibition that the person to whom the data is released or disclosed may not further use, release or disclose such data, and the contractor or subcontractor or subcontractor asserting the restriction is notified of such release, disclosure or use. This legend, together with the indications of the portions of this data which are subject to such limitations, shall be included on any reproduction hereof which includes any part of the portions subject to such limitations.

THIS TECHNICAL REPORT HAS BEEN REVIEWED AND IS APPROVED FOR PUBLICATION.

Earl Shultz, LTC, MS 166401

REPORT DOCUMENTATION PAGE			Form Approved OMB No. 074-0188	
Public reporting burden for this collection of information is estimated to average 1 hour per response, including the time for reviewing instructions, searching existing data sources, gathering and maintaining the data needed, and completing and reviewing this collection of information. Send comments regarding this burden estimate or any other aspect of this collection of information, including suggestions for reducing this burden to Washington Headquarters Services, Directorate for Information Operations and Reports, 1215 Jefferson Davis Highway, Suite 1204, Arlington, VA 22202-4302, and to the Office of Management and Budget, Paperwork Reduction Project (0704-0188), Washington, DC 20503				
1. AGENCY USE ONLY (Leave blank)	2. REPORT DATE January 2001	3. REPORT TYPE AND DATES COVERED Annual (1 Jan 00 - 31 Dec 00)		
4. TITLE AND SUBTITLE Template Based Design of Anti-Metastatic Drugs from the Active Conformation of Laminin Peptide II		5. FUNDING NUMBERS DAMD17-97-1-7207		
6. AUTHOR(S) Jean R. Starkey, Ph.D.				
7. PERFORMING ORGANIZATION NAME(S) AND ADDRESS(ES) Montana State University Bozeman, Montana 59717-2470 E-Mail: umbjs@gemini.oscs.montana.edu		8. PERFORMING ORGANIZATION REPORT NUMBER		
9. SPONSORING / MONITORING AGENCY NAME(S) AND ADDRESS(ES) U.S. Army Medical Research and Materiel Command Fort Detrick, Maryland 21702-5012		10. SPONSORING / MONITORING AGENCY REPORT NUMBER		
11. SUPPLEMENTARY NOTES This report contains color photos				
12a. DISTRIBUTION / AVAILABILITY STATEMENT Distribution authorized to U.S. Government agencies only (proprietary information, Jan 01). Other requests for this document shall be referred to U.S. Army Medical Research and Materiel Command, 504 Scott Street, Fort Detrick, Maryland 21702-5012.			12b. DISTRIBUTION CODE	
13. ABSTRACT (Maximum 200 Words) Major advances were made towards elucidating the structure of the ligand-binding domain of the 67 kDa LBP. Phage display studies indicated that three sequence domains in the C-terminal domain of the LBP likely interact with peptide 11. Both GB1 fusion domains and other cohesive domains of LBP, identified by limited proteolysis studies, have been expressed in recombinant bacterial systems. Well-dispersed NMR spectra have been generated for several of these, indicating that they will be useful for structure determination of the LBP ligand-binding domain. We now have a successful synthetic path for the candidate 16 YIGSR mimetic, which was designed by an early run of the INVENTON program. On receipt of sufficient material, this will shortly be investigated for its bioactivity. Structurally related compounds will be used in structure:activity studies to optimize the bioactivity of the mimetic. To facilitate the preclinical studies, metastatic variants of the MDA-MB-231 and MDA-MB-435 human breast cancer cell lines have been generated. Since we have found that LBP shedding is estrogen responsive, we have also derived more invasive variants of the T47D ER+ve breast cancer cell line. The LBP protein was shown to have a sulfhydryl oxidase activity, and facilitated peptide 11 dimerization.				
14. SUBJECT TERMS Breast Cancer			15. NUMBER OF PAGES 47	
			16. PRICE CODE	
17. SECURITY CLASSIFICATION OF REPORT Unclassified	18. SECURITY CLASSIFICATION OF THIS PAGE Unclassified	19. SECURITY CLASSIFICATION OF ABSTRACT Unclassified	20. LIMITATION OF ABSTRACT Unlimited	

FOREWORD

Opinions, interpretations, conclusions and recommendations are those of the author and are not necessarily endorsed by the U.S. Army.

___ Where copyrighted material is quoted, permission has been obtained to use such material.

___ Where material from documents designated for limited distribution is quoted, permission has been obtained to use the material.

___ Citations of commercial organizations and trade names in this report do not constitute an official Department of Army endorsement or approval of the products or services of these organizations.

X In conducting research using animals, the investigator(s) adhered to the "Guide for the Care and Use of Laboratory Animals," prepared by the Committee on Care and use of Laboratory Animals of the Institute of Laboratory Resources, national Research Council (NIH Publication No. 86-23, Revised 1985).

X For the protection of human subjects, the investigator(s) adhered to policies of applicable Federal Law 45 CFR 46.

X In conducting research utilizing recombinant DNA technology, the investigator(s) adhered to current guidelines promulgated by the National Institutes of Health.

X In the conduct of research utilizing recombinant DNA, the investigator(s) adhered to the NIH Guidelines for Research Involving Recombinant DNA Molecules.

N/A In the conduct of research involving hazardous organisms, the investigator(s) adhered to the CDC-NIH Guide for Biosafety in Microbiological and Biomedical Laboratories.

 22-01
PI - Signature Date

Table of Contents

Report Documentation Page	2
Foreword	3
Table of Contents	4
Introduction	5
Body of Report	6
Figure 1	8
Figure 2, Figure 3	9
Figure 4	10
Figure 5, Figure 6	11
Figure 7	15
Figure 8, Figure 9	20
Figure 10, Figure 11	21
Figure 12, Figure 13	22
Table 1, Table 2	23
Conclusions	24
Key Research Accomplishments	25
Reportable Outcomes	27
References	28
Salaried Individuals	30

Introduction

Many clinical studies on breast cancer and other solid tumors show strong positive correlations of high expression of the 67 kDa laminin binding protein (LBP) with poor prognosis^{1,2,3,4,5,6,7,8,9,10,11}, and, more recently, results from SAGE studies which are available on the internet confirm this correlation for colon cancer. The 67 kDa LBP has been shown to be a legitimate target for cancer therapy by the demonstration that reduction of tumor cell expression of the 67 kDa LBP, brought about by anti-sense or antibody approaches does inhibit tumor metastasis in mice^{12,13,14}. However, current limitations with gene and antibody therapies restrict the use of these approaches for long term clinical applications. Our approach is to use the active conformation of the matrix ligand for the 67 kDa LBP as a template for the design of orally compatible anti-metastatic drugs. This ligand has been identified as a nine amino acid sequence from laminin-1, CDPGYIGSR, and is known as peptide 11^{15,16}. The actual mimetics are designed to represent only the YIGSR region of bound peptide 11, because YIGSR is known to be the minimal active sequence¹⁶ and synthesis of organic mimetics for longer sequences than this is daunting.

The ability of synthetic peptide 11 or YIGSR to block tumor cell invasion and metastasis depends on its ability to interfere with the interactions of the 67 kDa LBP with basement membrane laminin-1^{15,16}. The 67 kDa LBP (a dimer from the 37 kDa LBP gene product) derives from the S2 ribosomal class of proteins¹⁷, a unique evolution having occurred in the C-terminal domain in parallel with the appearance of laminin and laminin-like molecules¹⁷. This C-terminal domain has been indicated by us and others as the matrix ligand binding domain^{18,19,20,21}. The half-life of peptide 11 (and YIGSR) in the bloodstream is in the order of minutes, consistent with rapid proteolysis²². Therefore, in order to develop useful therapeutics, either the biological half-life of peptide 11 must be very significantly extended, or else it is essential to mimic the properties of peptide 11 using non-peptide compounds. The overall goal of this research project is to design accurate mimetics using template -based approaches, and to evaluate their anti-invasive and anti-metastatic activity. If we are successful in synthesizing mimetics with good anti-metastatic activity, this will provide a "proof of concept" for our structure -based design approach, and the best mimetics should be effective lead compounds suitable for going into combinatorial chemistry programs to provide the most effective derivatives.

There are three specific aims which should allow us to accomplish the goal of this research project:

Aim 1 In collaboration with Drs. V. Copié and E. A. Dratz, of the Chemistry and Biochemistry Department at MSU¹, to determine the relevant structural characteristics of the ligand-binding domain of the LBP.

Aim 2 In collaboration with Dr. W. Todd Wipke, Professor of Chemistry and Biochemistry, UCSC², to undertake structure-based design of non-peptide mimetics for the active conformation of peptide 11 using INVENTON, an artificially intelligent computer program for the design of structural mimetic compounds.

Aim 3 In collaboration with Dr. J. Konopelski, UCSC, to synthesize the most promising structures derived by the INVENTON program, and to evaluate the activities of the new compounds in inhibiting tumor cell invasion *in vitro*, and metastasis in experimental animals.

¹ MSU = Montana State University

² UCSC = University of California, Santa Cruz

Body of Report

This is a highly collaborative project with contributions from five different laboratories and two different institutions. It follows that the "statement of work" is complex, and for convenience of the reader, we re-iterate it below.

STATEMENT OF WORK:

Technical Objective (aim) 1

- Task 1: Months 1-15: Determine the LBP residues which interact with peptide 11.
- Task 2: Months 1-18: Express the ligand binding domain of the LBP in *E. coli*, conduct multidimensional NMR experiments to determine structural information relevant to drug design.
- Task 3: Months 1-15: Provide all relevant information from Tasks 1-2 of this proposal, along with the fully refined bound peptide 11 conformation (**derived from work carried out exclusively on our NIH award**), to Dr. Wipke to improve the peptide 11 template used by INVENTON for the design of peptide mimics.

Technical Objective (aim) 2

- Task 4: Months 6-18: Using the artificially intelligent program, INVENTON, design mimics of the LBP-bound conformation of peptide 11 (actually the YIGSR domain from this structure).
- Task 5: Months 12-18: Integrate new information coming from tasks 1-3 into the drug design template used by INVENTON.
- Task 6: Months 6-18: Evaluate the output structures from INVENTON for potential drug lead compounds. Synthesize the most approachable of these.
- Task 7: Months 6-18: Work with Dr. Wipke's group in providing heuristic rules for determining the relative ease of synthesis for output structures from INVENTON.
- Task 8: Months 12-22: Provide Dr. Starkey's group with mimetic compounds for limited preclinical tests.

Technical Objective (aim) 3

- Task 9: Months 1-12: Test informative analogs of peptide 11 for anti-invasive and anti-metastatic activity.
- Task 10: Months 12-24: Test mimetic compounds for 1) tissue culture toxicity, 2) anti-invasive activity and 3) anti-metastatic activity.

Progress on Technical Objective 1, task 1.

Experimental Methods and Procedures

The methodology originally outlined in the grant application was restricted to mapping the contact residues in the LBP by using our photo-crosslinking biotinylated analog of peptide 11²³. The derivatized LBP and its cleavage fragments would be isolated using monovalent avidin matrices, and final analysis would be carried out using mass spectrometry sequencing techniques. The proposed methodology for isolating derivatized LBP and cleavage products relied on the use of commercially available monovalent avidin matrices. Unfortunately, these gave very poor yields and commercial anti-biotin antibodies were found to exhibit very low affinities. We, therefore, made our own rabbit anti-biotin antibodies for this work. Appropriate antibody specificity was sought using immunizing antigens consisting of biotin and biotinylated peptide 11 crosslinked to an irrelevant protein (KLH - keyhole limpet hemocyanin). After removal of KLH specific responses, we tested the antibodies by Western blot analysis. Good titers were found to biotinylated proteins and derivatized LBP. The antibody still exhibited unwanted cross reactions and was further purified over a peptide 11 column to provide a highly specific reagent capable of isolating derivatized LBP from detergent extracts of tumor cell membranes. Unfortunately, yields of derivatized LBP from whole cell membranes were still relatively low, and we decided to utilize rLBP instead for these experiments.

Because of the initial difficulties with isolating sufficient derivatized LBP from tumor cell membranes, we carried out a series of experiments using phage display mapping to identify sequences within the LBP which interact with peptide 11. This alternative experimental approach cannot provide the detail to identify the actual contact residues, but, nonetheless, provided very useful preliminary data identifying the interacting sequences. The results of this work were published in the Journal of Molecular Biology. *Reprints of this manuscript are included with this final report, and the reader is referred to them for detailed methods, results and discussion.*

Limited proteolysis experiments were carried out on isolated recombinant LBP using trypsin and elastase. Both proteases yielded useful sized fragments which were purified by HPLC and then sequenced. Interestingly, surface exposed (detectable early in the time course) cleavage sites were found in all regions which were predicted by our phage display mapping experiments to interact with peptide 11. The same cleavage, isolation and sequencing experiments are being completed on photocrosslinked rLBP. Mapping of peptide 11 contact residues in rLBP will not be completed within the time frame of this award, but will be completed under the American Cancer Society grant awarded to Dr. Copié last year.

Assumptions

We anticipated that results from the phage display experiments would identify sequences within the LBP which contain the contact residues for peptide 11.

Results

Specifically eluted phage populations exhibited three classes of mimotopes for different regions in the cDNA derived amino acid sequence of the 67 kDa laminin binding protein (LBP). These regions were 1) a palindromic sequence known as peptide G, 2) a predicted helical domain corresponding to LBP residues 205-229, and 3) TEDWS -containing C-terminal repeats. All elution conditions also yielded phage with putative heparin binding sequences. We modeled the LBP²⁰⁵⁻²²⁹ domain, which we demonstrated by

circular dichroism (CD) to have a helical secondary structure, and determined that this region likely possesses heparin binding characteristics located to one side of the helix, while the opposite side may contain a hydrophobic patch where peptide 11 could bind. Using Elisa plate assays, we demonstrated that peptide 11 and heparan sulfate both individually bound to synthetic LBP²⁰⁵⁻²²⁹ peptide. We also demonstrated that synthetic PATEDWSA peptide could inhibit tumor cell adhesion to laminin-1. These data support the proposal that the 67 kDa LBP can bind the β -1 laminin chain at the peptide 11 region, and suggest that heparan sulfate is a likely alternate ligand for the binding interactions. Our results also confirm previous data¹⁹ suggesting that the most C-terminal region of the LBP, which contains the TEDWS repeats, is involved in cell adhesion to laminin-1, and we specifically indicated the repeat sequence in that activity. For details of this work, the reader is referred to the copies of our publication in J. Mol. Biol. submitted with this report.

Limited proteolysis experiments, carried out on well folded samples of rLBP, demonstrated that all three regions indicated by the phage display experiments as interacting with peptide 11, were on the surface of the protein. This data strongly supports our interpretation of the phage display results and is included in a manuscript currently in preparation (see next section).

Discussion and Recommendations

These experiments indicate that peptide 11 interacts with three different sequences domains in the 67 kDa LBP. The data also suggests that heparin/heparan sulfate is an alternate ligand for the 67 kDa LBP. As expected, the ligand binding domain of the LBP appears to be quite complex. Any structures developed for the active conformation of peptide 11, and for the ligand binding domain of the LBP, need to be compatible with these data on peptide 11 interacting sequences.

Progress on Technical Objective 1, task 2.

Experimental Methods and Procedures

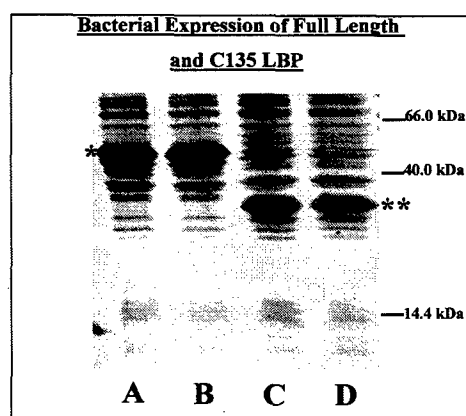


Figure 1. Whole bacterial cell lysates resolved on Coomassie Blue stained SDS-PAGE gels. Asterisks indicate the positions of the recombinant LBP products.

Expression of the ligand binding domain of the LBP in *E. coli*:

This work is being carried out in collaboration with Dr. Valérie Copié at Montana State University. The first step in conducting the NMR structural studies of the ligand binding domain of the LBP was to express this domain in bacteria. This allows for heavy isotope labeling of the domain at reasonable cost. The coding region for the full length expression product was obtained from our mammalian vector and initially cloned into the pTrcHis B prokaryotic expression vector (Invitrogen). Top 10 *E. coli* cells (Invitrogen) were successfully transformed, and they produced a protein of the correct molecular weight which stained positively with our anti-LBP antibody in a Western blot. However, the Trp

promoter in this vector is not particularly efficient, and only modest yields of the LBP were obtained.

A second vector was then tried. This is the pET-30 vector from Novagen which utilizes the more efficient T7 promoter system. This time, we used CD41 *E.*

coli cells which have been successfully used in our hands to produce isotopically labeled peptides. On induction with IPTG (Isopropyl- β -D-thiogalactopyranoside), large quantities of the expressed LBP were obtained (Figure 1), and the same was the case for the C135 LBP ligand binding domain. We utilized the N-terminal poly-His tag for isolation of the expressed recombinant protein by Ni affinity (Figure 2). The pET-30 vector contains two N-terminal protease cleavage sites for removing the poly-His tag. Closest to

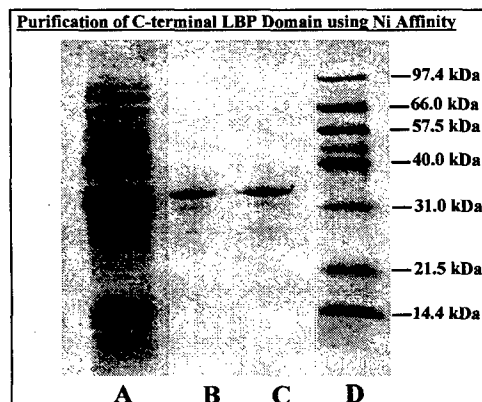


Figure 2. Purification of C135 LBP expression product using Ni affinity. SDS-PAGE gel stained with Coomassie Blue. Lane A = whole cell lysate, lanes B and C = imidazole eluate from the Ni column, lane D = molecular weight markers.

the expressed protein sequence is an enterokinase site. We abandoned this site when we could not achieve cleavage efficiencies greater than 50%. The more distant thrombin cleavage site worked very well with close to 100% efficiency (Figure 3). Biotinylated thrombin is used for the cleavage, and it is easily removed from the expressed protein preparation over a streptavidin column. Free poly-His sequence is removed by a second pass over the Ni column. While, the pET-30 vector system worked well for our protein, the expression product contained too many extra residues. Therefore we eventually utilized a modification of this vector, pET-15b which does not contain an enterokinase cleavage site, and which has the thrombin cleavage site immediately N-terminal to the expressed protein sequence. The molecular weight of the isolated expressed C135 ligand binding domain was checked by time of flight MALDI (matrix assisted laser desorption) mass spectrometry, and the success of refolding the domain by circular dichroism (CD) spectroscopy.

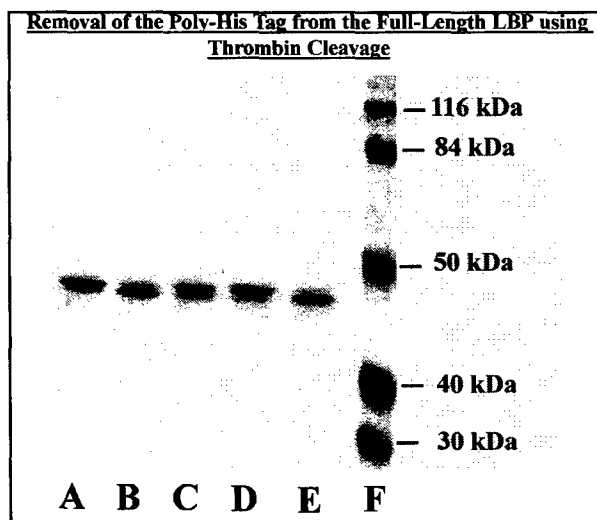


Figure 3. Full length LBP bacterial product resolved on a Coomassie Blue stained SDS-PAGE gel. Lane A = uncut product, lanes B-D = product partially cleaved by thrombin, lane E = fully cleaved product, lane F = molecular weight standards.

The recombinant C135 domain labelled well with ^{15}N , a prerequisite for NMR studies. However, while this domain remained well folded at low and medium concentrations, at the high concentrations needed for NMR structure determination, partial aggregation was noted. Comparisons between native and reduced gels indicated that aggregation was in part driven by disulfide bond formation occurring between LBP molecules. We mutated the two Cys residues in the LBP to Ala. The Cys minus expression product did not aggregate as badly as the wild type protein, however, aggregation still made NMR work problematical. Two other approaches were

used to improve the solubility status of the LBP products. The limited proteolysis experiments were used to identify more cohesive domains for expression, and LBP domains have been expressed as mosaics with the streptococcal protein G GB1 domain

to induce solubility in the experimental protein sequence²⁴. Well resolved spectra have been obtained from some of the domains identified by limited proteolysis.

Assumptions

The only assumption being made for this task is that the bacterial monomeric protein will function like the high molecular weight form of the protein. The only published data indicate that, for binding to laminin-1, this is true²⁸. Unsupported statements (no data given) in the literature question this finding²⁹. Therefore, we conducted a series of control binding experiments with the monomer. These studies indicated that the recombinant monomer bound to laminin-1 in a qualitatively similar way to the shed 67 kDa LBP. However, the avidity of binding was greater for the 67 kDa mammalian form of the protein LBP.

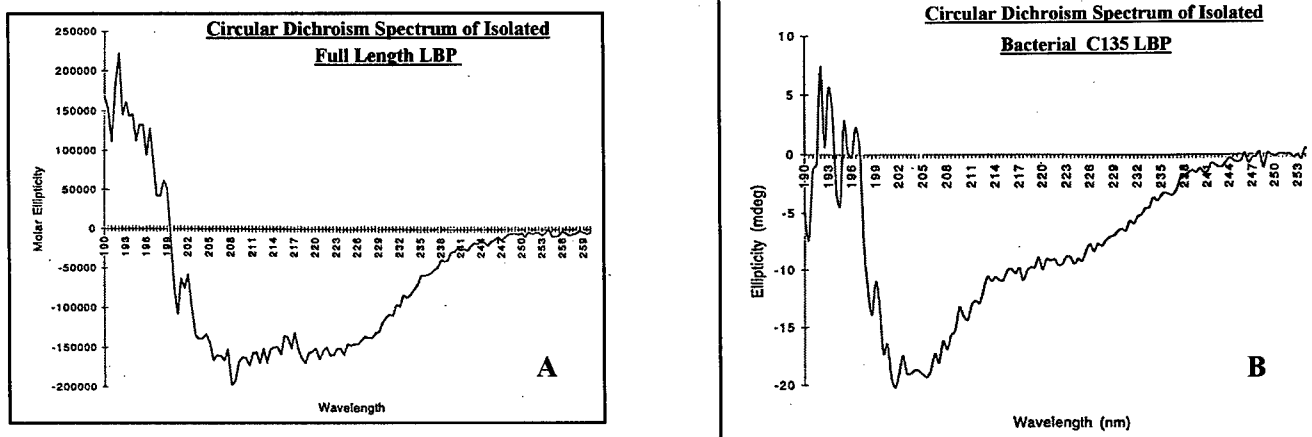


Figure 4. Circular Dichroism Spectra for (A) isolated mammalian 67 kDa LBP, and (B) recombinant C135 LBP matrix ligand binding domain.

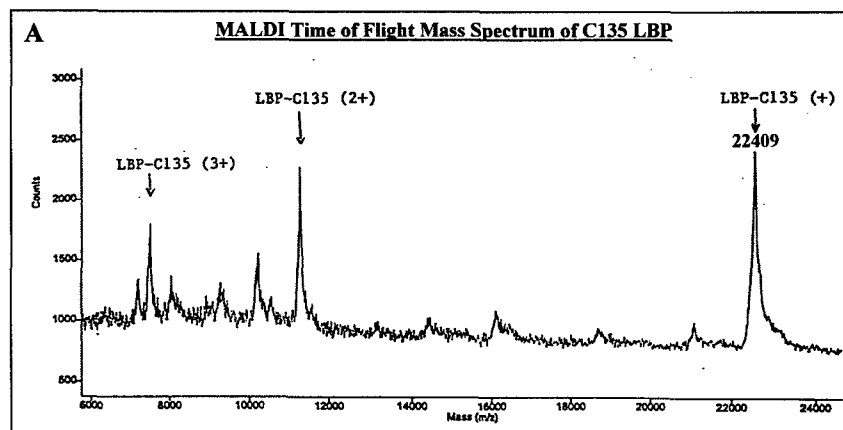


Figure 5. Mass Spectrometry analysis of the C135 LBP domain.

(Figure 3).

After refolding the initially denatured bacterial expression product, most of the CD spectra showed no evidence of random coil structure indicating adequate refolding. The LBP CD spectrum is dominated by an alpha helical profile. Since the majority of the predicted alpha helix is in the C-terminal domain of the protein, we expect a largely alpha helical profile for the C135 LBP domain also. Figure 5 shows the mass spectrum obtained for the isolated C135 LBP domain. Both full length rLBP (Figure 6) and C135 LBP were shown to bind to laminin-1 in ELISA assays. Aggregation of the recombinant C135 LBP domain at NMR concentrations was shown to be partially driven by disulfide bond formation, and approaches have been taken to alleviate this problem. In the last year of the project, we discovered that we could generate a 67 kDa form of the LBP from

bacteria when expression was allowed to take place at 15 degrees C rather than room temperature. Comparisons between the bacterial and the mammalian 67 kDa proteins are currently underway. *A manuscript is currently in preparation which describes the limited proteolysis studies, the generation of recombinant LBP domains and preliminary NMR spectra.*

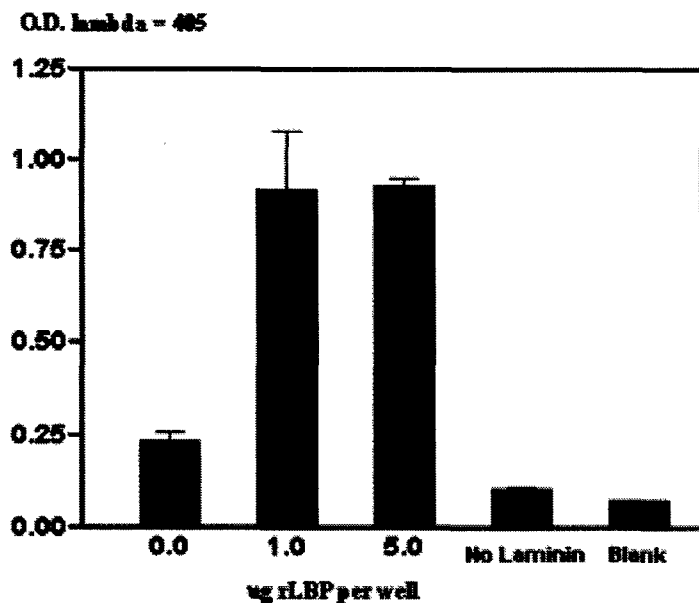


Figure 6. ELISA assay showing binding of laminin-1 to rLBP.

Results

As discussed in the "Methods" section, we have succeeded in generating efficient bacterial expression systems for full length LBP, the C135 ligand binding domain (Figure 1), and several of the fragments identified via limited proteolysis. The expressed proteins are readily purified over Ni columns using imidazole elution (Figure 2), and the poly-His sequence is efficiently removed using thrombin

Discussion and Recommendations

The current bacterial expression systems are working well, and can be used to provide heavy isotope labeled C135 LBP product and other fragments for the NMR experiments. Partial aggregation of the LBP and its fragments at the high concentration needed for NMR work continues to be an annoyance. However, the improved solubility of some of the new

fragments as well as the GB1 fusion constructs are sufficient to allow for NMR structural work. The structural work is being completed under the ACS award to Dr. Copié.

Progress on Technical Objective 1, task 3.

Experimental Methods and Procedures

Although structural work on peptide 11 is exclusively supported by our NIH award, the data it provides is used in this Army project. Therefore, a brief update of the relevant findings are provided here.

Information about the orientation of required amino acid sidechains in the peptide 11 template is critical to the design of active peptido-mimetics. Unfortunately, there are few NMR crosspeaks to the required Tyr, Ile or Arg sidechains in aqueous solution. We took advantage of the fact that the relatively viscous DMSO solvent would slow down the motion of the peptide and allow for better definition of individual structure conformations in NMR experiments.

In this solvent we found a sufficient number of long range cross-peaks to allow for structure determination of the shorter YIGSR peptide. The two-dimensional NMR spectra run in DMSO provided a greatly increased number of crosspeaks, with several additional $i,i+2$ backbone NOEs over those seen in the aqueous spectra. $i,i+2$ backbone NOE crosspeaks were found for C-terminal amide to serine, arginine to glycine and serine to isoleucine. The NMR spectra suggested that a water molecule stabilizes the YIGSR peptide by interacting with the tyrosine and the serine hydroxyl residues. Considering all our data, particularly the earlier structure:function studies with numerous peptide 11 analogs³⁰, we concluded that the DMSO structure for the YIGSR peptide was likely different from the receptor bound conformation in water. This could either result from "induced fit" on binding, or from DMSO structures being inherently different from the aqueous ones.

Assumptions

We assumed that the structure of the peptides in DMSO would be similar enough to the aqueous structures to provide useful information. The validity of this assumption varies with different peptide sequences, but we suspect that the assumption may not hold for peptide 11 or YIGSR. However, if the assumption is good, then there must be induced fit of the docking YIGSR sidechains upon receptor binding. Knowing that such a situation could exist may greatly facilitate future optimization of YIGSR mimetics.

Results

It appears that our original structure:function studies provide the most useful information to date for mimetic design. The DMSO structures for YIGSR fail to present the required sidechains in the manner expected from this earlier structure:function work. Thus, it may be that there is an induced fit of the peptide upon binding to the LBP protein. This would be very important information for future drug optimization.

Discussion and Recommendations

Our additional work on this objective has served to highlight the importance of the earlier structure: function studies on various peptide 11 analogs. It also highlights the importance of determining the structure of the ligand-binding domain of the LBP protein. We are pursuing the NMR studies to do this on the new ACS award, and we have added an X-ray crystallographic collaboration after learning that a Russian group had successfully crystallized the bacterial recombinant protein³¹.

Progress on Technical Objective 2, tasks 4 and 5.

Experimental Methods and Procedures

Structural information from the full peptide 11 sequence is utilized because the minimal active domain, YIGSR, is too small to provide sufficient NMR crosspeaks. However, only the structure coordinates etc. for the YIGSR region are used in the drug design process. This provides a reasonably sized template for the design of non-peptide mimetics. Design of potential mimetics is carried out using the artificially intelligent program, INVENTON. The pharmacophore hypothesis provides the computer program with information as to what aspects of the peptide were likely important in recognition and binding with the LBP. The receptor (LBP) sees the shape of the peptide, and interacts with its electron density and dipolar nature. For template-based design, INVENTON uses the field of the template. Clearly, candidate structures must have chemically stable functionality. They must also survive the human digestive system to allow for oral therapy.

Now that we are working to obtain an NMR and/or X-ray determined structure defining the ligand binding domain of the LBP, we will be able to incorporate characteristics of the LBP binding pocket in mimetic design. This was the original way INVENTON was used. The computer algorithms design specific mimics for the detailed bound structure completely automatically using FASM, fragment assembly for construction. After all structures are ranked, individual candidates are examined and molecular dynamics simulations are performed to evaluate flexibility and the ability of the molecule to retain the desired conformation. Dr. Konopelski is responsible for evaluating the probable ease of synthesis of mimetics, and for choosing the actual synthetic approaches.

Assumptions

The main assumption in this part of the work is that the program INVENTON will design mimics which are at least as good as those designed by a human chemist. Our experience with the program working on other projects is that this is the case. Furthermore, the program is far more innovative, producing structures pharmaceutical chemists would not because of the biases in their training and professional experience.

Results

Dr. Wipke's group has been working on refining the operation of the INVENTON program, in particular attempting to automate aspects of ranking the prolific output of mimetic structures for ease of synthesis. We have experienced problems designing synthetic pathways for INVENTON's innovative structures. Indeed, this is the reason why this project could not be completed on time. Candidate 16 looked quite approachable and turned out to be very challenging.

Discussion and Recommendations

We now have a successful path to the synthesis of the first mimetic designed by INVENTON (candidate 16 - Figure 7). Once sufficient compound is available (currently being produced), for the preclinical work to be completed in the Starkey lab, we will be able to ascertain whether we are close to our goal of providing a sufficiently active lead compound, or whether major modifications will be needed. Future runs with INVENTON will incorporate structural information from the binding pocket of the LBP. We will optimize the mimetic after ascertaining the bioactivity of the numerous structurally related compounds being produced in the Konopelski lab.

Progress on Technical Objective 2, tasks 6,7 and 8.

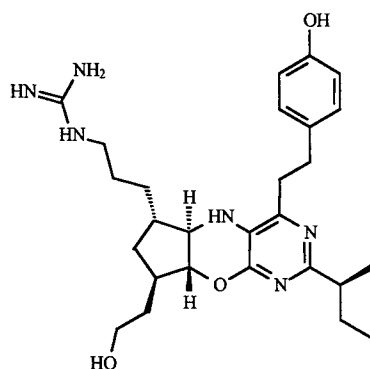


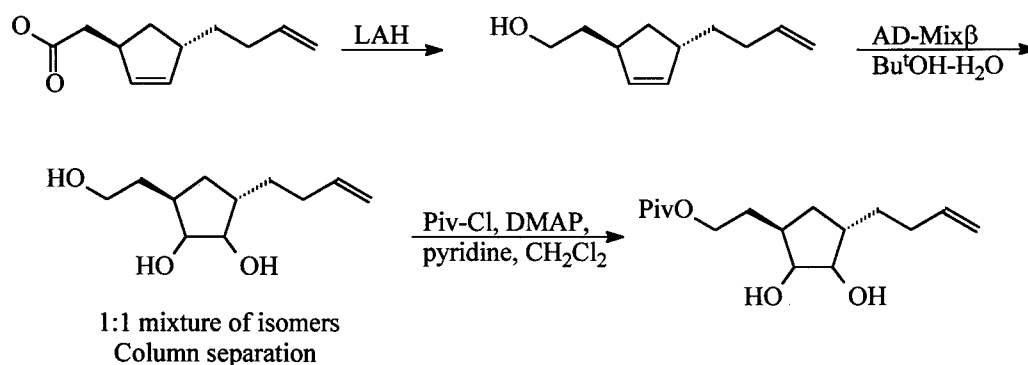
Figure 7. Candidate 16

The Konopelski team at UCSC continues to work toward the production of sufficient **candidate 16** YIGSR mimetic for preclinical testing in the Starkey lab. This compound was initially designed by the Wipke team using the INVENTON suite of programs. The synthetic work was approached from a drug discovery point of view, with the emphasis on the production of a series of structurally related compounds that can afford excellent structure/activity data after testing. The challenge of forming the tricyclic core structure has finally been met, and the last few steps to producing testable quantities of the desired material are currently underway. INVENTON designs mimetics *de novo*

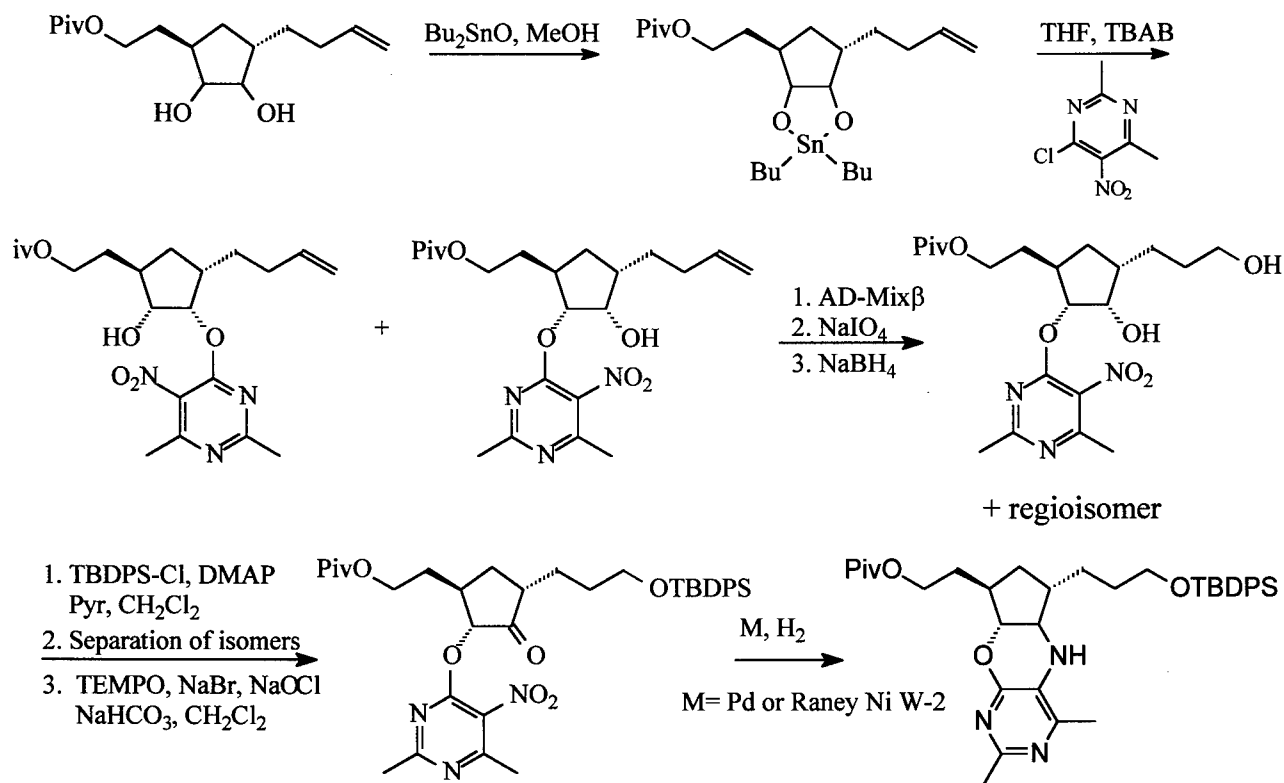
without the bias resulting from the experience of a pharmaceutical chemist. Judging the ease of synthesis of such compounds is problematical even for a very experienced chemist. Candidate 16 proved to be surprisingly challenging, and, as indicated in the earlier reports, the first approaches did not work. Below is an outline of the successful synthetic design:

Synthesis of the Carbocyclic Unit

The cyclopentane ring of the desired compound derives from a known compound. Dihydroxylation affords a 1:1 mixture of isomers, which can be separated by column chromatography.

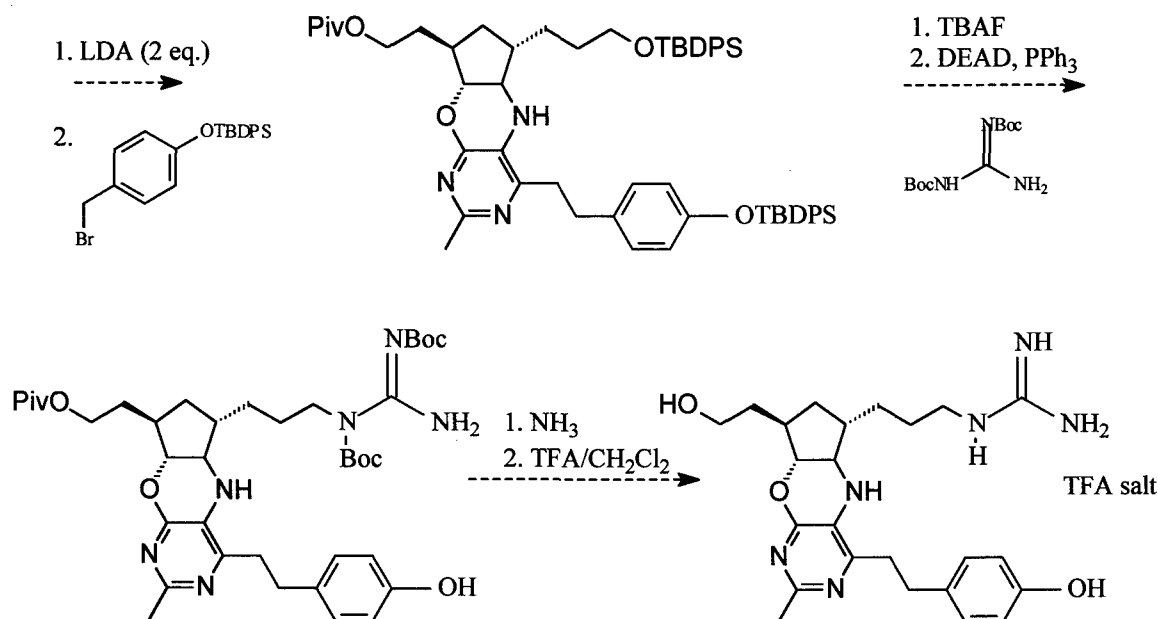


Coupling to the Pyrimidine Unit and Formation of the Tricyclic Core



Independently, the isomers are reacted with a pyrimidine unit through the formation of a tin ketal, which renders a bound oxygen nucleophilic. The reaction affords a mixture of regioisomers which cannot be separated without further equilibration. After much experimentation, a suitable procedure for elaboration of the alkene side chain to the alcohol of desired length and formation of the cyclopentanone group was discovered. Further experimentation was required to obtain the desired selectivity in reduction of the nitro group of the pyrimidine ring to the corresponding amine. This reaction is accompanied by condensation of the amine with the ketone to afford the imine, which is reduced to the desired morpholine ring.

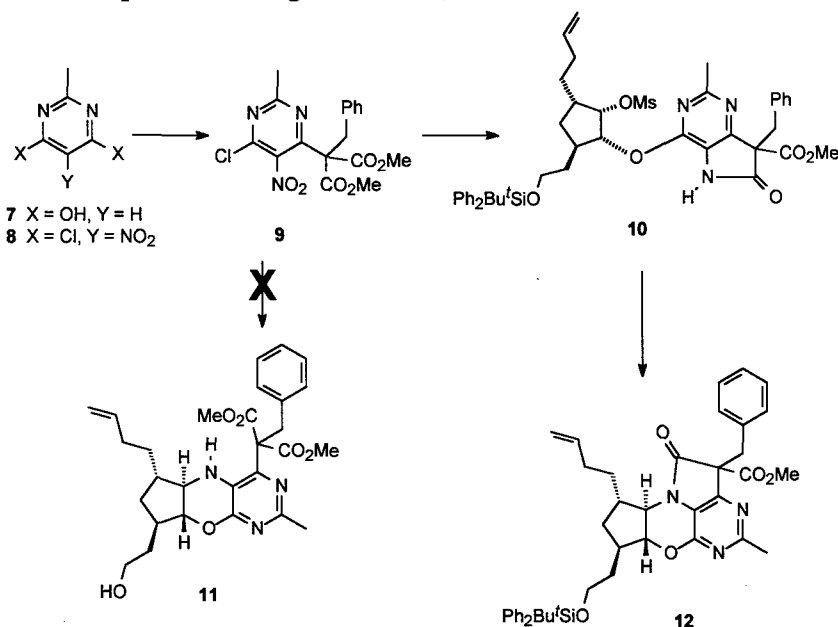
Final Elaboration to the Desired Product



Synthesis of Candidate 16 is completed by introduction of the tyrosine side chain and elaboration of the arginine side chain.

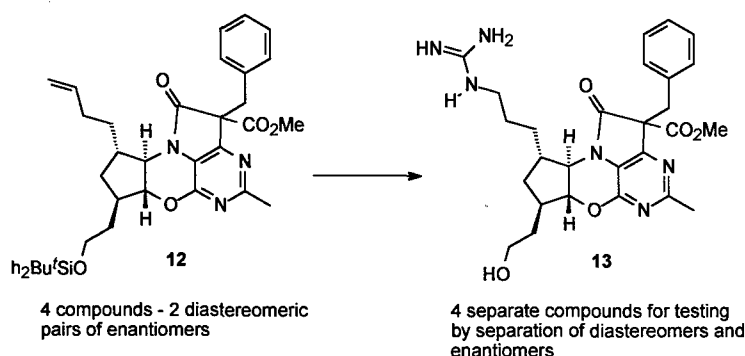
Synthesis of a Series of Structurally Related Compounds to Refine the Optimal Geometry for Anti-invasive Activity

Results from the Starkey lab suggested that the isoleucine side chain might act to reduce the conformational flexibility of the tyrosine aromatic ring, thereby positioning the phenol functionality in the proper space for binding. Given that **candidate 16** provides a rigid scaffold, the isoleucine side chain is not strictly required. Therefore, we prepared our first compound for testing from commercially available **7** as indicated in the diagram to the left. Mesylate formation and reduction of the nitro group affords lactam **10** as a separable mixture of diastereomers rather than tricycle **11**. Treatment of **10** with base affords tetracyclic **12**, which has the desired scaffold in place *and holds the tyrosine side chain more rigidly than does candidate 16*. Removal of the protective groups and elaboration of the guanidine functionality will afford one of



the early compounds to be tested in the Starkey laboratory.

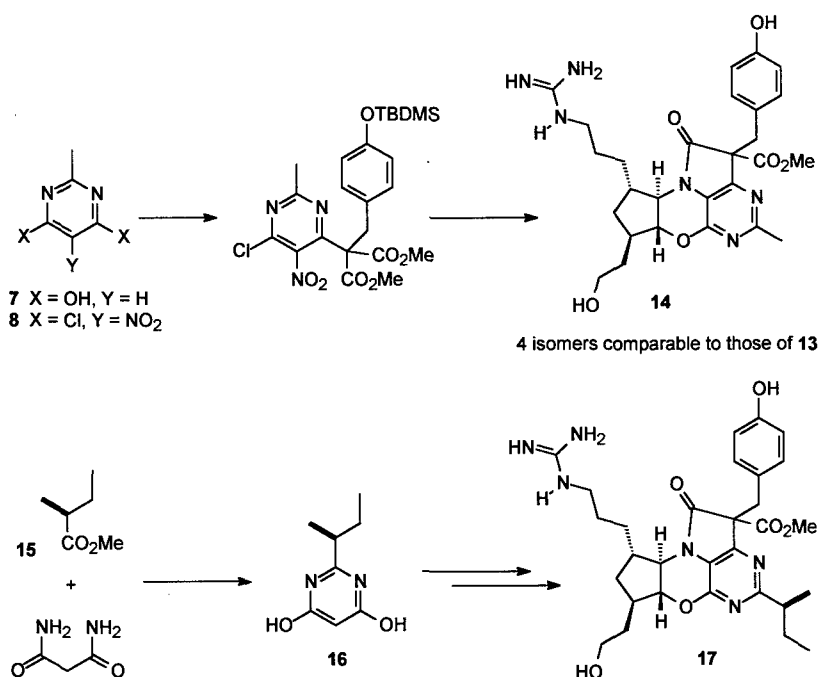
With the synthesis of compound **12**, the route to a variety of materials based on the **candidate 16** structure is secure. Our plan is to generate a variety of closely related compounds in quick succession so as to produce a body of testing data. These data will then be evaluated to provide insights into structure-activity relationships and guide our future synthetic efforts to even more active compounds (i.e. optimization).



Our plan calls for completion of the synthesis of **13** from **12**. This transformation will lead to four compounds, since **12** is actually a mixture of 2 diastereomers, each of which is a mixture of enantiomers. The diastereomers of **12** are easily separable by simple column chromatography, so each isomer is individually taken on to tetracycle **12**.

A key compound is **14**, in which the phenyl ring is replaced by a phenol to afford a true tyrosine-type functionality.

Compound **17** possesses the complete side chain array of **candidate 16**, but in addition has the lactam and ester. We have not attempted to remove these extraneous groups since the lactam brings two additional benefits to the design of **candidate 16**; namely, the extra rigidity in the tyrosine side chain and the presence of an additional chiral center. The ability to separate the diastereomers generated by this new chiral center will allow for a fine-tuning of the phenol position in a way that is not possible with the more mobile ethylene chain of **candidate 16**.



Assumptions

None

Results

A successful synthetic design has been produced for Candidate 16. As soon as we have sufficient material, this mimetic will go into preclinical testing against human breast cancer cell lines in the Starkey lab. This will include anti-invasive and anti-metastatic testing in *SCID* mice. Closely related compounds having several chiral centers have also been synthesized. The various stereoisomers can be individually isolated for structure:activity relationship studies. This will greatly facilitate the design of second generation mimetics. The University of California, Santa Cruz has started the process of patenting both the design methodology and Candidate 16. This is essential for any further drug development.

Discussion and Recommendations

Computer *de novo* design of mimetic structures has one major difficulty. That is: ranking the ease of synthesis of a very large number of candidate compounds (about 2000 per run). In fact, this is the most active area of research for the INVENTON program at this time. Candidate 16 appeared to be readily accessible, but proved to be a major challenge. However, it should be noted that our very small collaborative group was attempting to synthesize a mimetic compound where a drug company would have used many more people working in parallel. It is significant that we succeeded in synthesizing our target compound at a fraction of the cost which traditional approaches would have incurred. It took us much longer than we anticipated, and almost all of the preclinical testing will happen after the DOD support for this project has expired. Nevertheless, as an idea project, we are happy with the outcome: a successful design for the synthesis of Candidate 16 was found, and a number of structurally related compounds were synthesized. Patent considerations require that biological activity is shown for Candidate 16 during the next 6 months, and this is now considered a priority by both collaborating universities.

Progress on Technical Objective 3, task 9.

Experimental Methods and Procedures

Anti-invasive activity of peptide 11 and its analogs/mimetics is tested using an in vitro two-chamber "Transwell" assay³². An 8 μ m pore size polycarbonate filter separating the upper and lower chambers of a 6.5 mm Transwell (Costar) is impregnated with a 1:20 dilution of Matrigel. 5×10^4 tumor cells are added to the upper well in 0.2 ml complete medium, and 0.8 ml complete medium was added to the lower well, and medium was changed daily. Incubation of the "Transwells" is continued for 3 days and cells invading into the bottom well are quantitated using the colored MTT (3-[4,5-Dimethylthiazol-2-yl]-2,5-diphenyltetrazolium bromide) metabolite.

The lung colony assay is used to evaluate anti-metastatic activity. Tumor cells are harvested from subconfluent cultures with minimal trypsin/EDTA exposure. Prior to injection, mice are warmed at 37°C for 30 minutes. A set number of monodispersed tumor cells are injected per mouse in 0.2 ml via the lateral tail vein. Where the experiment requires co-injection of tumor cells with peptide, cells are prepared as indicated above. One mg peptide dissolved in the injection buffer is first loaded in 0.1 ml into the syringe, then the aliquot of tumor cells added in a further 0.1 ml. The contents of the syringe are

gently mixed by inversion and injected as described above. The mice are killed several weeks later and autopsied. All tissues with suspect tumor colonies are rinsed in PBS and fixed in Bouin's fixative for gross and histological examination. The number of superficial nodules in the Bouin's-fixed tissues are determined using a dissecting microscope.

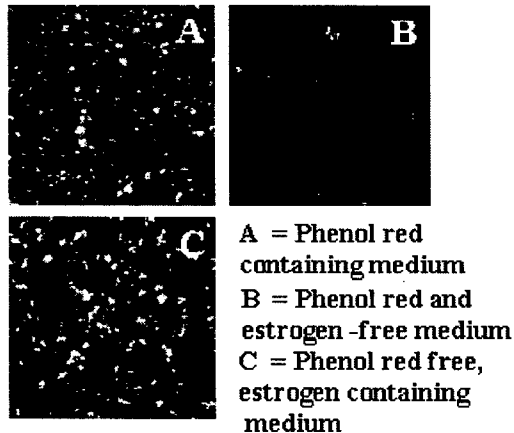


Figure 8. Confocal micrograph of shed LBP, bound to matrix laminin-1 and visualized using avidin-FITC. Laminin-1 substrate was exposed to 24 hour conditioned medium from CHO cells.

We have also subjected the ER +ve human breast cancer cell line, T47D, to selection for a more metastatic phenotype by a combination of *in vivo* passage and selection for the ability to invade through Matrigel basement membrane matrix *in vitro*. The time to first observation of invaded cells in the transwell assay indicates the success of the selections. For T47D cells which were selected *in vitro*, this time shortened from 10 days to 4 days to 2 days for the three rounds of selection. For T47D cells which had been serially passaged three times in the mammary fat pad of *SCID* mice, invaded cells were first seen at 2 days, and their frequency was higher than was the case for the cells only selected *in vitro*. The ER status of the selected variants is currently being determined. So long as the cells are still ER +ve, they should provide useful variants for the preclinical studies. Since we have determined that shedding of the LBP molecule is estrogen responsive (Figs 8,9), it is important to test mimetics against both ER +ve and ER -ve breast cancer cell lines.

Assumptions

The general, and unavoidable, assumption made with the animal experiments is that human breast cancer cells will behave in *SCID* mice in the same way as they do in the human patient. There is also an assumption made that the "Transwell" *in vitro* invasion assay will reasonably predict anti-metastatic activity. After many years of experience with both assays, we are confident that the two assays give roughly parallel results for the type of work being done on this project. Certainly, the *in vitro* assay is a useful screen before going into animal experiments.

While we conducted most of our preliminary work with standard rodent test cell lines, we are now working exclusively with human breast cancer cell lines. For the MDA-MD-453 and MDA-MD-231 cell lines, *SCID* mice are employed for the experimental metastasis assays. We selected variants of both the MDA-MD-453 and MDA-MD-231 cells by serial lung colony development in *SCID* mice. The selected variants reproducibly develop high numbers of lung metastases after intravenous injection. Both of these lines are estrogen receptor (ER) negative.

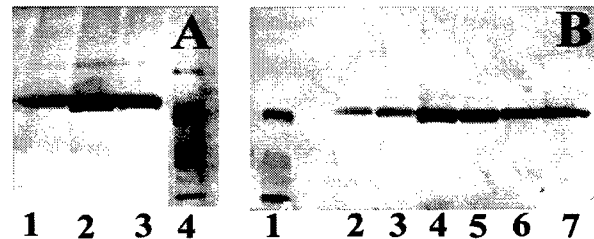


Figure 9. Silver stained SDS-PAGE gel of shed LBP affinity isolated from 3ml MCF-7 (A) and OVCAR (B) cell conditioned medium. Lanes 1A,3B= 10-7M, lanes 2A,4B= 10-8M and lanes 3A,5B= 10-9 M 17 β estradiol.

Results

The NMR experiments, carried out under our NIH award, to determine the active conformation of peptide 11 utilized Tr-NOESY (Transferred Nuclear Overhauser Effect Spectroscopy) experiments where the peptide interacted with purified LBP. Dithiothreitol is used to prevent dimerization of free peptide 11, but was not used in the presence of the LBP which has an internal disulfide bond. Detailed examination of Tr-NOESY spectra revealed that the bound conformation of peptide 11 was dominated by a structure which could not be distinguished from synthetic peptide 11 disulfide dimer. Since peptide 11 can spontaneously dimerize under the conditions used in these NMR experiments, the presence of peptide 11 dimer was initially viewed simply as an unwanted complication.

N-acetyl -peptide 11 was found to dimerize very much more slowly than non acetylated peptide 11 in the absence of dithiothreitol (7-10 days compared with 6-7 hours for peptide 11 at room temperature at pH = 5.0). Surprisingly, N-acetyl -peptide 11 dimerized rapidly in the presence of the 67 kDa LBP.

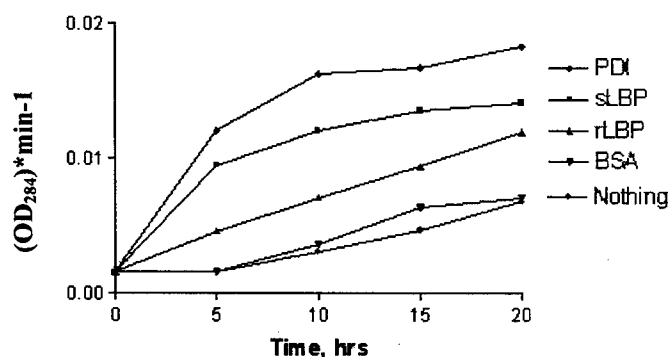


Figure 10. RNAase A refolding assay for sulfhydryl oxidase activity. RNAase activity assayed for 20 hours of refolding using 2':3'-cyclic cytidine monophosphate

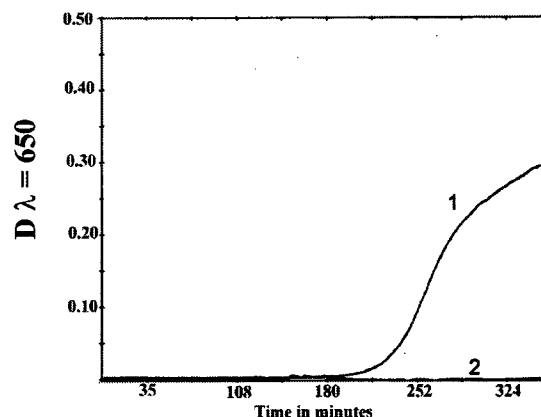


Figure 11. DTT driven Insulin reduction. 1 – no sLBP present. 2 – in the presence of 1.5 μM sLBP

Rapid dimerization occurred when the N-acetyl -peptide 11 was present in 32 fold excess of concentration over the LBP, and the rate of dimerization was found to increase with increasing concentration of the LBP. Enzymatic activity of the 67 kDa LBP was suspected, and after appropriate controls were carried out, this was confirmed. Thus, the 67 kDa LBP appears to have a sulfhydryl oxidase activity. This activity was demonstrated for shed LBP isolated from conditioned tissue culture medium, for LBP isolated from EHS basement membrane matrix and for recombinant protein expressed in *E. Coli*. We have succeeded in demonstrating that LBP can facilitate the refolding of denatured RNAase A (Fig. 10), but inhibits the reverse reaction of reducing and denaturing insulin (Fig. 11). The sulfhydryl oxidase activity is most pronounced for the shed LBP (Fig 10).

Since the two Cys residues in the LBP protein are separated by 13 residues, there is no canonical CXXC motif as would be expected for a classical protein disulfide isomerase. Also, as indicated above, we could not demonstrate any induced disulfide reduction attributable to the LBP protein. Therefore, LBP does not appear to be a protein disulfide isomerase. The mechanism of the sulphydryl oxidase activity is still unclear, but we have shown that FAD does not facilitate the reaction. We mutated the Cys residues in rLBP to Ala, both singly and together, and examined the effects on RNAase A refolding. The mutant with no Cys residues was least active, while the mutant proteins with only one Cys residues were of intermediate activity. Therefore, while the Cys residues appeared to be important, we could not

demonstrate an intermediate with the expected molecular weight of a mixed disulfide species as would be expected for a protein disulfide isomerase. Therefore, it may be that loss of the internal disulfide bond, which is known to be present in the LBP molecule, changes the conformation of the protein sufficiently to reduce the enzymatic activity.

Our current hypothesis is that shed LBP could facilitate tumor cell invasion. Preliminary experiments, quantitating invasion of DG44CHO cells through basement membrane matrix *in vitro*,

Invasion of DG44CHO cells through Matrigel Basement Membrane Matrix in 3 days

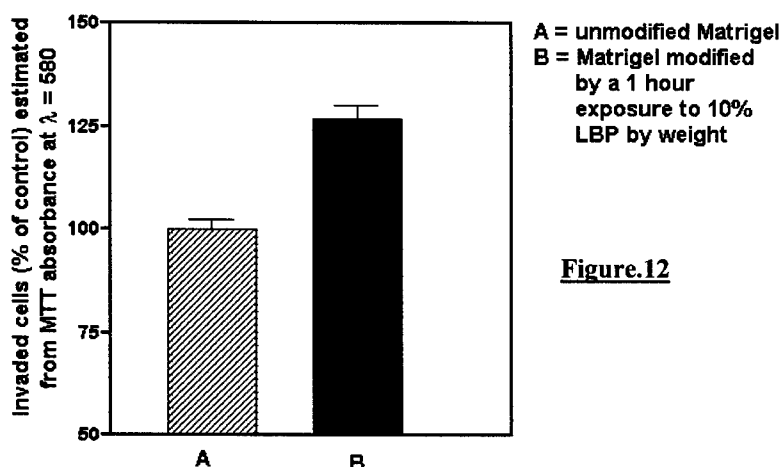


Figure.12

revealed a significant increase of invasion over three days for matrix pretreated with 67 kDa LBP (Figure 12.). Addition of shed or recombinant LBP to the medium in Transwell assays also increased invasion of human ovarian carcinoma cells (Figure 13). Given the preliminary data indicating that dimerization of peptide 11 might be involved in the bioactivities of the peptide, we compared the bioactivities of peptide 11, a non-oxidizable

monomer of peptide 11 containing an AcM protected cysteine residue and peptide 11 dimer. The disulfide dimer was slightly more active *in vitro* (anti-invasion) and *in vivo* (anti-metastatic) compared to peptide 11, but significantly more active than the AcM protected peptide 11 monomer (Table 1., Table 2.). The AcM protected monomer was the least active in each case.

Invasion of Matrigel Basement Membrane by NIH OVCA Cells in one week

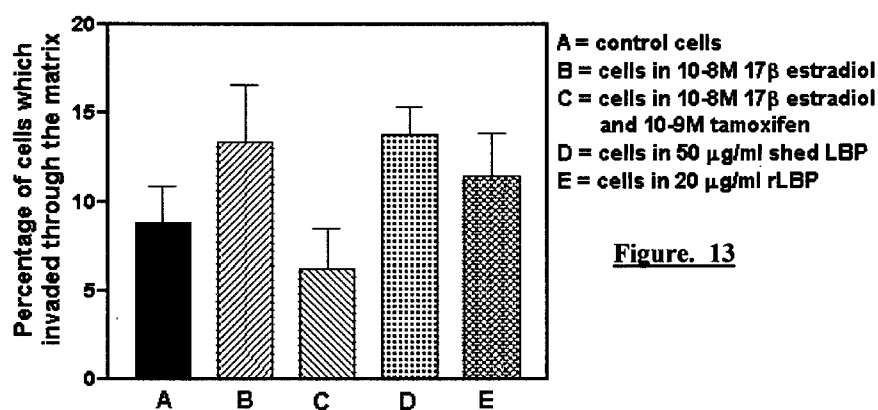


Figure. 13

Table 1. - Effect of Monomeric and Dimeric Peptide 11 on CHODG44 Cell Invasion of Matrigel Basement Membrane Assayed using the In Vitro Transwell Assay

Peptide ¹	% Inhibition of Invasion
Peptide 11	51.2 \pm 3.6
Acm-peptide 11	11.4 \pm 10.1
Peptide 11 dimer	75.7 \pm 4.1

¹100µg peptide per ml medium.

²Each data point represents 6 replicates.

Table 2. - Effect of Monomeric and Dimeric Peptide 11 on Experimental Metastasis Formation by B16BL6 Cells

Peptide ¹	% Inhibition of metastasis	p value ²
None	None	-
Peptide 11	45	0.017
Acm-peptide 11	20	0.154
Peptide 11 dimer	51	0.007

¹1mg peptide used per mouse.

²Mann-Whitney U 2-tailed test. ³n=7 mice.

Discussion and Recommendations

While any experimental data shedding light on the possible mechanisms of action of the 67 kDa LBP in facilitating tumor cell invasion and metastasis is very welcome, the sulphydryl oxidase activity of the protein does complicate the structural studies being carried out on the NIH award. Fortunately, the dimer is symmetrical, so all our previous structural work on peptide 11 is valid. Since the minimal active sequence of peptide 11, YIGSR, is just as active as peptide 11 itself, YIGSR is still viewed as the most appropriate template for drug design. We expect to be able to elucidate why this short sequence is so active when we have determined the NMR structure of the LBP ligand binding domain. Most likely, the longer peptide requires interactions with the LBP at the N-terminal Cys residue as well as docking via the Tyr and Arg sidechains. The smaller YIGSR peptide may be able to fit into the binding pocket without the Cys interaction.

Progress on Technical Objective 3, task 10.

Work on this task will commence with the receipt of a sufficient amount of candidate 16 by the Starkey lab. *The University of California, Santa Cruz has started the process of patenting candidate 16 so that further development, which would require the involvement of a drug company, can go forward. UCSC does not usually initiate patenting without financial input from an interested commercial concern, so the action is considered an unusually aggressive move on the part of the university. Montana State University has provided a loan to the Starkey lab to facilitate the completion of this task after the expiration of the DOD award.*

Conclusions

Although difficulties with our isolation procedures for ligand derivatized LBP slowed down studies identifying contact residues for peptide 11 in the LBP ligand binding domain, the alternative approach of using phage display studies to pinpoint regions of interacting sequence worked very well. The phage display studies indicated that three separate sequence domains in the C-terminal domain of the LBP could interact with peptide 11, and this work has been published in the *J. Mol. Biol.* Also, limited proteolysis studies on rLBP were found to be consistent with results from the phage display mapping.

In order to undertake NMR studies of the structure of the ligand binding domain of the LBP at reasonable cost, the binding domain needed to be expressed in a recombinant bacterial system. We have accomplished this for the full length protein, for the C135 ligand binding domain and for several other domains which were indicated by the limited proteolysis studies. LBP domains have also been expressed in vectors (obtained from the NIH) which produce the domain linked by the N-terminus to the GB1 domain of staphylococcal protein G. The highly soluble GB1 domain greatly facilitates initial NMR studies. The *E. coli* strains used, express large amounts of poly-His tagged protein which is readily purified over a Ni affinity column. The poly-His tag is removed using thrombin cleavage, and the molecular weights of the expression products were confirmed by mass spectrometry. As judged by circular dichroism studies, the majority of the recombinant proteins and domains refolded well. Initial NMR spectra are well dispersed for several of the expression products, but even with eliminating the possibility of disulfide driven aggregation, product aggregation is still an annoyance at very high protein concentrations. However, useful spectra have been collected for some LBP domains. We have also initiated a collaboration to do an X-ray structure of the recombinant protein since initial crystallization conditions have been worked out by Sorokin et al. Using both structural approaches, we are confident that the LBP ligand binding domain will be solved.

We now have a successful synthetic route for candidate 16, a mimetic which was designed by one of the early runs of the artificially intelligent INVENTON program. This last summer we thought that we had a correct tricyclic structure, only to find that the chirality of one region was incorrect after NMR analysis. This setback required the design of yet another synthetic approach, fortunately a successful one. The Konopelski lab will provide sufficient material to the Starkey lab for bioactivity testing very shortly. The results of these tests are very important, as they will indicate if the designed mimics are close to a potential drug lead, or if major modification to the INVENTON pharmacophore hypothesis will be needed. Two sources of additional information will guide future work to optimize the mimetic. One will be our structural studies of the ligand binding domain of the LBP, and the other the results of structure:activity studies on the many compounds which are structurally related to candidate 16 and which have been synthesized in the Konopelski lab. The University of California, Santa Cruz has initiated the patent process for candidate 16 and for the design process which was used. This opens the way to further drug development.

The difficulties encountered in designing a successful synthetic protocol for candidate 16 underscored a potential problem with artificial intelligent mimetic design. The INVENTON program is quite prolific in the number of candidate structures it produces. While it is relatively easy to rank these based on fit with the pharmacophore hypothesis, it is very hard to accurately rank them for ease of synthesis. Partly as a result of the difficulties we encountered, the most active area of research for the INVENTON project is currently how to do this type of ranking. Nevertheless, it must be pointed out that we have derived a mimetic and a successful synthetic protocol to make this mimetic at a fraction of the costs which standard approaches would have incurred.

Because some of our initial experiments indicated that the 67 kDa LBP had a sulphhydryl oxidase activity and could facilitate dimerization of peptide 11, we compared the anti-invasive and anti-metastatic activity of peptide 11, a non oxidizable AcM protected analog of peptide 11 and peptide 11 dimer. The most active species was the dimer, with the AcM protected monomer being the least active in each case. Interaction with the LBP via the N-terminal Cys residue is likely to be important to ligand binding of the longer peptide 11, while it appears not to be so for the short, very active, YIGSR peptide. Any structure which we derive for the "binding pocket" of the LBP will need to be compatible with these results.

We have selected human ER -ve breast cancer cell lines for reproducible metastatic behavior in *SCID* mice. This was required for preclinical testing of YIGSR mimetics. We have determined that LBP shedding is estrogen sensitive and that shed LBP may facilitate invasion. To explore this further, we have spent a significant effort selecting appropriate estrogen receptor positive breast cancer cell lines. Therefore, we are now in a position to evaluate our YIGSR mimetics against both ER +ve and ER-ve human breast cancer cells.

Key Research Accomplishments

- **Successfully identified regions in the LBP protein which interact with peptide 11 using phage display and limited proteolysis experiments.**
- **Successfully expressed full length LBP, the ligand binding domain, and GB1 fusion domains of the LBP in *E. Coli*.**
- **Successfully labelled rLBP with heavy isotopes for NMR spectroscopy.**
- **Determined which recombinant LBP domains give well dispersed preliminary NMR spectra, and so can be used for structure determination.**
- **Determined a successful synthetic approach for Candidate 16.**

- Synthesized a number of close structural relatives to Candidate 16 which will be useful for structure:activity studies to determine the optimal geometry for bioactivity.
- Selected variants of the MDA-MB-435 and MDA-MB-231 ER-ve human breast cancer cell lines which reproducibly produce good numbers of experimental lung colonies in *SCID* mice.
- Selected more invasive variants of the ER+ve T47D human breast cancer cell line to facilitate preclinical testing of mimetics.
- Determined that cell shedding of the LBP is sensitive to estrogen levels in ER+ve breast and ovarian cancer cell lines, and that this may be related to the ability of shed LBP to facilitate invasion *in vitro*.
- Determined that the LBP has a sulfhydryl oxidase activity, and that dimerization of peptide 11 may be related to its bioactivity.
- Initiated the process of patenting candidate 16.

Reportable Outcomes:

1. Three manuscripts have been published and a fourth is *in preparation* at this time.

Kazmin, D.A., Hoyt, T.R., Taubner, L., Teintze, M., and Starkey, J.R. Phage Display Mapping for Peptide 11 -Sensitive Sequences Binding to Laminin-1. *J. Mol. Biol.* 298:431-445, 2000.

Starkey, J.R., Uthayakumar, S., Berglund, D.L. Cell surface and substrate distribution of the 67-kDa laminin binding protein determined by using a ligand photoaffinity probe. *Cytometry* 35:37-47, 1999.

Starkey, J.R., Dai, S., Dratz, E.A. Sidechain and backbone requirements for anti-invasive activity of laminin peptide 11. *Biochim. Biophys. Acta* 1429:187-207, 1998.

2. One presentation was given at the 98 AACR annual meeting, a presentation was given at the 2000 "Era of Hope" meeting, and two invited seminars were given (Chemistry Department, University of California, Santa Cruz; NIH, NIAID Hamilton, MT).
3. A new grant, based on work started under this award, has been obtained by Dr. Copié from the American Cancer Society. One other research grant application is pending.

Title = NMR Structure Determination of the Ligand-binding Domain of the 67 kDa
Laminin Binding Protein
Agency = ACS
2 year award which activated Jan 1, 2000
Total award = \$380,000

4. One of the predoctoral students working on this project has received a \$30,000 dissertation award from the Komen Foundation.
5. Three predoctoral students, and one postdoctoral fellow, have worked on this project.

References

1. G. De Manzoni et al., *Oncology (Basel)* 55, 456-460 (1998).
2. M. I. Colnagi, *Adv. Exp. Med. Biol.* 353, 149-154 (1994).
3. K. Satoh et al., *Biochem. Biophys. Res. Commun.* 182, 746-752 (1992).
4. X. Sanjuán et al., *J. Pathol.* 179, 376-380 (1996).
5. M. G. Daidone, R. Silvestrini, E. Benini, W. F. Grigioni, A. D'Errico, *Br. J. Cancer* 76, 52-53 (1997).
6. G. Gasparini et al., *Int. J. Cancer* 60, 604-610 (1995).
7. D. Waltregny, L. De Leval, S. Ménard, J. De Leval, V. Castronovo, *Journal of the National Cancer Institute* 89, 1224-1227 (1997).
8. G. Pelosi et al., *J. Pathol.* 183, 62-69 (1997).
9. F. A. Van den Brule et al., *Eur. J. Cancer* 30A, 1096-1099 (1994).
10. P. Viacava et al., *J. Pathol.* 182, 36-44 (1997).
11. D. P. Pei, Y. Han, D. Narayan, D. Herz, T. S. Ravikumar, *J. Surg. Res.* 61, 120-126 (1996).
12. K. Mafune and T. S. Ravikumar, *J. Surg. Res.* 52, 340-346 (1992).
13. K. Narumi et al., *Jpn. J. Cancer Res.* 90, 425-431 (1999).
14. K. Satoh et al., *Br. J. Cancer* 80, 1115-1122 (1999).
15. J. Graf et al., *Cell* 48, 989-996 (1987).
16. Y. Iwamoto et al., *Science* 238, 1132-1134 (1987).
17. E. Ardini et al., *Mol. Biol. Evol.* 15, 1017-1025 (1998).
18. T. H. Landowski, U. Selvanayagam, J. R. Starkey, *Clin. Exp. Metastasis* 13, 357-372 (1995).
19. J. Yannariello-Brown, U. Wewer, L. Liotta, J. A. Madri, *J. Cell Biology* 106, 1773-1786 (1988).

20. V. Castronovo, G. Taraboletti, M. E. Sobel, *Cancer Res.* 51, 5672-5678 (1991).
21. K.-S. Wang, R. J. Kuhn, E. G. Strauss, S. Ou, J. H. Strauss, *J. Virol.* 66, 4992-5001 (1992).
22. Y. Kaneda et al., *Invasion Metastasis* 15, 156-162 (1995).
23. J. R. Starkey, S. Uthayakumar, D. L. Berglund, *Cytometry* 35, 37-47 (1999).
24. J. R. Huth, et al, *Protein Sci* 6, 2359 (1997).
25. G. Taraboletti, D. Belotti, R. Giavazzi, M. E. Sobel, V. Castronovo, *JNCI* 85, 235-240 (1993).
26. N. Guo, H. C. Krutzsch, T. Vogel, D. D. Roberts, *J. Biol. Chem.* 267, 17743-17747 (1992).
27. U. M. Wewer, G. Taraboletti, M. E. Sobel, R. Albrechtsen, L. A. Liotta, *Cancer Res.* 47, 5691-5698 (1987).
28. E. Y. Siyanova, *Bulletin of Experimental Biology and Medicine* 113, 70-72 (1992).
29. R. P. Mecham, *FASEB J.* 5, 2538-2546 (1991).
30. J.R. Starkey, S. Dai, E.A. Dratz, *Biochim. Biophys. Acta* 1429, 187 (1998).
31. A. V. Sorokin, et al, *Biochemistry (Moscow)* 65, 644 (2000).
32. L. A. Repesh, *Invasion and Metastasis* 9, 192-208 (1989).

Salaried personnel:

Dr. Jean R. Starkey
Dr. Edward A. Dratz
Dr. Mahesh Jaseja
Deborah Berglund
Dmitri A. Kazmin
Laura Taubner
Stephanie Hopkins

JMB



**Phage Display Mapping for Peptide 11 Sensitive
Sequences Binding to Laminin-1**

**Dmitri A. Kazmin, Teri R. Hoyt, Lara Taubner, Martin Teintze
and Jean R. Starkey**

Phage Display Mapping for Peptide 11 Sensitive Sequences Binding to Laminin-1

Dmitri A. Kazmin¹, Teri R. Hoyt², Lara Taubner¹, Martin Teintze¹ and Jean R. Starkey^{2*}

¹Department of Chemistry and Biochemistry and

²Department of Microbiology Montana State University Bozeman, MT 59717, USA

We utilized a 9-mer random phage display library to identify sequences which bind to laminin-1 and elute with heparan sulfate or peptide 11 (CDPGYIGSR). Laminin-1 derivatized plates were used for biopanning. Three consecutive rounds of low pH elutions were carried out, followed by three rounds of specific elutions, each consisting of a heparan sulfate elution followed by a peptide 11 elution. The random sequence inserts were sequenced for phage populations eluted at low pH, by heparan sulfate and by peptide 11. Specifically eluted phage populations exhibited three classes of mimotopes for different regions in the cDNA derived amino acid sequence of the 67 kDa laminin binding protein (LBP). These regions were (1) a palindromic sequence known as peptide G, (2) a predicted helical domain corresponding to LBP residues 205–229, and (3) TEDWS-containing C-terminal repeats. All elution conditions also yielded phage with putative heparin binding sequences. We modeled the LBP^{205–229} domain, which is strongly predicted to have a helical secondary structure, and determined that this region likely possesses heparin-binding characteristics located to one side of the helix, while the opposite side appears to contain a hydrophobic patch where peptide 11 could bind. Using ELISA plate assays, we demonstrated that peptide 11 and heparan sulfate individually bound to synthetic LBP^{205–229} peptide. We also demonstrated that the QPATEDWSA peptide could inhibit tumor cell adhesion to laminin-1. These data support the proposal that the 67 kDa LBP can bind the β -1 laminin chain at the peptide 11 region, and suggest that heparan sulfate is a likely alternate ligand for the binding interactions. Our results also confirm previous data suggesting that the most C-terminal region of the LBP, which contains the TEDWS repeats, is involved in cell adhesion to laminin-1, and we specifically implicate the repeat sequence in that activity.

© 2000 Academic Press

Keywords: 67 kDa laminin binding protein; phage display; laminin-1; peptide 11; haparan sulfate

*Corresponding author

Introduction

Many clinical studies on solid tumors show a strong positive correlation of high expression of

Abbreviations used: LBP, 67 kDa laminin binding protein; GAG, glycosaminoglycan; LE, laminin epidermal growth factor like repeat; CD, circular dichroism; MTT, 3-[4,5-dimethylthiazol-2-yl]-2,5-diphenyltetrazolium bromide; PFU, plaque forming unit; BSA, bovine serum albumin; BLAST, Basic Local Alignment Search Tool; standard single and three letter codes are used for amino acid residues.

E-mail address of the corresponding author: umbjs@gemini.oscs.montana.edu

the 67 kDa LBP with poor prognosis (De Manzoni *et al.*, 1998; Colnagi, 1994; Satoh *et al.*, 1992; Sanjuán *et al.*, 1996; Daidone *et al.*, 1997; Gasparini *et al.*, 1995; Waltregny *et al.*, 1997; Van den Brule *et al.*, 1994; Viacava *et al.*, 1997; Pei *et al.*, 1996). The 67 kDa LBP was originally described as “the laminin receptor”, but, with the subsequent description of laminin binding integrin receptors, the apparent common intracellular trafficking (Romanov *et al.*, 1994) and co-overexpression of the LBP and the α 6 β 1 integrin in some solid tumors (Halatsch *et al.*, 1997), as well as a demonstrated association of the 67 kDa LBP with the α 6 β 4 integrin (Ardini *et al.*, 1997), it is now considered much more likely that

the LBP modulates cell:basement membrane adhesion rather than mediating it. The fact that the LBP is shed from tumor cells in culture in large amounts proportional to the invasive potential of the cells (Karpatová *et al.*, 1996; Starkey *et al.*, 1999), and subsequently binds laminin-1 containing matrix substrates (Starkey *et al.*, 1999), is most consistent with an activity modifying cell: extracellular matrix interactions. The cDNA sequence of the LBP can only code for a non-glycosylated protein of about half the mass of that observed for the mature membrane and shed forms of the LBP. While the mature protein has been shown to be lipid acylated (Landowski *et al.*, 1995a; Butò *et al.*, 1998), studies by this lab (Landowski *et al.*, 1995a) and others (Castronovo *et al.*, 1991a) have failed to produce any evidence for N or O-linked glycosylation. There is experimental evidence that the high molecular weight mature form of the protein represents a dimer, but no conclusive evidence, as yet, demonstrating either a homo- or a hetero-dimer (Landowski *et al.*, 1995a; Rao *et al.*, 1989; Ménard *et al.*, 1997). The LBP cDNA sequence shares a very high homology with the S2 ribosomal class of proteins, so much so that the existence of functions for the LBP outside of those associated with ribosomal activities has been questioned by some investigators (Hung *et al.*, 1995). However, a detailed study of the evolutionary genomics of the 67 kDa LBP, revealed that a unique evolution of the protein occurred in the C-terminal domain in parallel with the appearance of laminin and laminin-like molecules (Ardini *et al.*, 1998). The subsequent very high conservation of this domain has the hallmark of the acquisition of a new and important function for the protein (Ardini *et al.*, 1998). Therefore, the most likely scenario is that the modern protein is multifunctional, having a role as a ribosomal protein (Ford *et al.*, 1999), and also having acquired a more recent function as a laminin binding protein (Ardini *et al.*, 1998). An interesting hypothesis is that the evolution of extracellular matrix binding activity could have occurred *via* a chaperone function for laminins (Ardini *et al.*, 1998). Two peptides derived from the C-terminal domain sequence, LBP residues 205-229 (Landowski *et al.*, 1995b) and LBP residues 161-180 (peptide G) (Magnifico *et al.*, 1996), have been shown to bind to laminin-1. In the case of peptide G, there is evidence that laminin-1 binding may be mediated *via* heparin or heparan sulfate (Guo *et al.*, 1992b). Potential involvement of heparin/heparan sulfate in laminin-1 binding by the LBP²⁰⁵⁻²²⁹ peptide, however, has not been evaluated to date.

Laminin-1 is one of the major components of basement membranes (Kleinman *et al.*, 1993). It is a large glycoprotein molecule (MW \approx 800 kDa), consisting of three polypeptide chains α 1, β 1 and γ 1, arranged in a characteristic cruciform shape. It contains multiple sites for polymerization, interaction with other components of basement membrane, such as collagen IV, nidogen and heparan sulfate proteoglycan (Kleinman *et al.*, 1982; Poschl *et al.*,

1996), as well as numerous cell adhesion molecules, such as integrins (Castronovo, 1993; Shaw & Mercurio, 1994) and non-integrin laminin receptors, including the 67 kDa laminin binding protein (LBP) (Yow *et al.*, 1988). Laminin-1 also contains numerous heparan sulfate/heparin-binding sites (Parthasarathy *et al.*, 1998; Hall *et al.*, 1997; Sung, 1997).

The peptide 11 sequence, CDPGYIGSR, which is found in the LE (laminin epidermal growth factor like) repeat region of the short arm of the β 1 laminin chain, was described as the ligand binding sequence for the 67 kDa LBP shortly after the initial descriptions of that protein (Graf *et al.*, 1987a,b; Iwamoto *et al.*, 1987). The proposed ligand function was deduced from the ability of the synthetic peptide to alter or mimic laminin-1 mediated cellular activities (Iwamoto *et al.*, 1988; Massia *et al.*, 1993). Associated with these activities were the ability to block tumor cell invasion of basement membrane, the ability to greatly reduce tumor lung colonization (Iwamoto *et al.*, 1987; Landowski *et al.*, 1995b), and the ability to block tumor angiogenesis (Sakamoto *et al.*, 1991). Anti-LBP antibodies have also been shown to interfere with cell spreading on immobilized YIGSR (Massia *et al.*, 1993). However, compelling proof of interaction of the 67 kDa LBP with laminin-1 at this site is still lacking. Indeed, rotary shadowing experiments appear to show a predominance of binding by the 67 kDa LBP to the long arm of laminin-1 just below the intersection of the cross (Castronovo, 1993). This is a short distance from the peptide 11 sequence in the short arm of the β 1 chain. Since the 67 kDa LBP has been shown to bind to laminin-1 via heparin or heparan sulfate (Guo *et al.*, 1992b), and since purified laminin-1 retains some heparan sulfate bound to it (Guo *et al.*, 1992b), the 67 kDa LBP is likely to be able to associate with isolated laminin-1 at more than one site *via* the residual laminin-bound glycosaminoglycan (GAG) moieties. Synthetic peptide 11, and its C-terminal YIGSR peptide, are currently being actively evaluated by several groups, including us, as potential anticancer drug leads (Starkey *et al.*, 1998; Nomizu *et al.*, 1993; Maeda *et al.*, 1998a,b). Should the peptide 11-containing domain of laminin-1 fail to interact in a major way with the 67 kDa LBP, then it would be essential to describe alternative amino acid sequences with which peptide 11 does show a significant interaction.

The current study uses phage display mapping to derive information about ligand binding interactions at the peptide 11 site in laminin-1. Since this sequence comprises only about 0.1% of the total length of the three chains of laminin-1, it was obvious that specific elution with free peptide 11 would be needed to enrich for phage whose binding to laminin-1 occurred in this region. Several experiments have been reported in which successful elution was performed using specific competition elution conditions instead of extreme pH (Pasqualini *et al.*, 1995; Ghossein *et al.*, 1997; Welply *et al.*,

1996). Our experimental design utilized three initial rounds of selection for phage exhibiting any type of binding affinity for laminin-1. This was accomplished with low pH elution which does not put any qualitative constraints on the nature of the binding. By initially eliminating all phage which failed to bind to laminin-1, we felt that this would favor the statistical likelihood of eventually isolating phage which bound to the peptide 11-containing LE repeat region.

In order to assess the biological relevance of the phage LBP mimotope sequences, we evaluated the ability of phage displaying LBP mimotopes to bind to isolated laminin-1. We also synthesized a peptide with the LBP homologous sequence of a repeatedly isolated mimotope, and tested its ability to inhibit cell adhesion to laminin-1. The nature of ligand interactions at the LBP²⁰⁵⁻²²⁹ domain was probed using (1) a photoactivatable crosslinking analog of peptide 11 (Starkey *et al.*, 1999) to assess the ability of peptide 11 to bind directly to the synthetic LBP²⁰⁵⁻²²⁹ helix peptide, and (2) using a sequence specific antibody for the LBP²⁰⁵⁻²²⁹ helix peptide (Landowski *et al.*, 1995b) to evaluate the ability of synthetic LBP²⁰⁵⁻²²⁹ peptide to bind to isolated heparan sulfate.

Results

Phage clones which bound to laminin-1 via peptide 11 sensitive mechanisms were obtained, but heparan sulfate binding phage clones could not be eliminated from the selected population

The bacteriophage display peptide library, J404 (DeLeo *et al.*, 1995), was screened for phage that selectively bound laminin-1 at the peptide 11, CDPGYIGSR, sequence. Our experimental design utilized multiple initial rounds of selection for phage with any type of affinity for laminin-1. These rounds were followed by specific elutions of laminin-1-bound phage with excess heparan sulfate then excess peptide 11. Titers of phage were obtained for all washes and eluates, providing information on the relative efficiency of heparan sulfate and peptide 11 elutions. Titers from the elution rounds 4, 5 and 6 showed that we succeeded in obtaining an enrichment for phage preferentially eluted by peptide 11. By round 5, peptide 11 eluted phage were substantially more

numerous than the mock buffer (Tris buffered saline) eluted phage, and this effect was maintained in round 6 (Table 1). The relative titers for elutions using heparan sulfate compared to the subsequent peptide 11 elutions are interesting because they stabilize by round 5. In the first round of the double specific selection (round 4), we found that the titer of phage in the heparan sulfate elution was 10.1 times higher than that in the peptide 11 elution. However, in round 5, this ratio decreased to 5.3, and in the sixth round was found to be essentially unchanged at 5.7 (Table 1). The proportional decrease in the numbers of phage which were eluted by heparan sulphate in the fifth round indicated that we had succeeded in reducing the contribution of heparan sulfate binding phage to the specifically eluted populations. However, in later rounds, we did not see any further relative decrease in the numbers of heparan sulfate-binding phage. Therefore, some fraction of the heparan sulfate sensitive binding appeared to be linked to peptide 11 sensitive binding.

To evaluate the overall specificity of the peptide 11 eluted phage sequences, starting with the low pH eluted phage population, three rounds of sequential heparan sulfate/peptide elutions were carried out using (1) scrambled peptide 11 (SRYDGGICP); (2) an unrelated bioactive laminin-1 peptide, AFSTLEGRPSAY (Ponce, *et al.*, 1999). For both of these control peptides, the contribution of heparan sulfate-binding phage to the final specific elution populations was very much smaller than was the case for the peptide 11 experiments. This finding supports specificity of the proposed link between heparan sulfate sensitive and peptide 11 sensitive phage binding.

Sequence analysis of specifically eluted phage reveals inserts with similarities for three regions of the 67 kDa LBP

We sequenced the recombinant inserts of 27 randomly picked phage clones eluted by heparan sulfate, as well as 66 phage clones eluted by peptide 11. Thirty eight of the peptide 11 eluted phage clones were from round 6, and 28 were from earlier rounds. In addition, we sequenced the inserts from 20 phage clones eluted by low pH during the initial three non-specific elutions, as well as inserts from 42 phage clones eluted by the irrelevant laminin-1 peptide and 41 phage clones eluted

Table 1. Comparisons of the numbers of phage specifically eluted from laminin-1 by heparan sulfate and by peptide 11 in the last three rounds of selection

	Round 4	Round 5	Round 6
% phage eluted by heparan sulfate	91	84	85
% phage eluted by peptide 11	9	16	15
% phage specific for peptide 11 ^a	1.2	18.5	42.3

Titers were derived from standard plaque forming assays using *E. Coli* K-91.

^a Calculated by subtracting the % phage eluted by TBS under identical conditions.

by scrambled peptide 11. The only informative sequences from the low pH eluted phage were five clones bearing inserts with two positively and no negatively charged residues (data not shown). Three of these sequences also contained tryptophan residues (data not shown). Heparan sulfate/heparin binding motifs are often characterized by an enrichment in basic amino acids juxta positioned to tryptophan residues (Guo *et al.*, 1992a; Cardin & Weintraub, 1989), and we concluded that these sequences likely represented heparan sulfate-binding peptides. Considering the fact that laminin-1 has numerous heparin/heparan sulfate binding sites, and isolated laminin-1 still has some residual glycosaminoglycan associated with it (Guo *et al.*, 1992b), recovery of potential heparin/heparan sulfate-binding sequences from the non-specific elutions was expected.

Table 2. shows informative phage sequences which were obtained from the specific elutions with peptide 11 and heparan sulfate. Phage clones carrying sequences mimicking three different regions of the 67 kDa LBP sequence were obtained. These regions are: the LBP²⁰⁵⁻²²⁹ putative helical domain, the LBP peptide G domain and the C-terminal DWS-containing repeats. Since antibodies have been independently raised to synthetic peptides containing the sequences of all three LBP regions (Wewer *et al.*, 1987; Landowski *et al.*, 1995b), the random phage displayed sequences which mimic these antigenic sequences can be classified as mimotopes. Amongst the sequenced inserts of the phage clones eluted by peptide 11 in round 6, we found six independent isolates

containing inserts coding for the sequence, KPWWRTINA, which shows a homology with the sequence of peptide G. Three individual isolates of phage carrying identical inserts coding for the sequence, QNTDWLGNL, were also identified from the round 6 peptide 11 elution. This sequence is reminiscent of the sequences of DWS-containing repeats which are found in the C-terminal portion of the 67 kDa LBP. The LBP peptide G region and the LBP²⁰⁵⁻²²⁹ domain have both been previously shown to be involved in binding to laminin-1, while an antibody, raised to the C-terminal LBP region containing the DWS repeats, modified cellular interactions with laminin-1. Our phage display results suggested that the DWS containing repeats could themselves bind to laminin-1. Heparan sulfate eluted numerous phage clones carrying sequences reminiscent of heparin/heparan sulfate-binding domains found in other proteins (Guo *et al.*, 1992a; Cardin & Weintraub, 1989) (Table 2). As indicated earlier, this was to be expected. Surprisingly peptide 11 was also quite efficient at eluting phage carrying these inserts, even in round 6 when the elution pattern had apparently stabilized. This suggests that some peptide 11 and heparan sulfate binding phage are interdependent in their binding to laminin-1. No phage insert sequences mimicking any LBP sequence domains were obtained with the irrelevant laminin-1 peptide, AFSTLEGRPSAY, while only a single sequence mimicking part of the LBP²⁰⁵⁻²²⁹ domain was obtained from the 41 sequenced phage clones eluted with scrambled peptide 11, SRYDGGICP. We were not surprised to obtain this mimic since a

Table 2. Sample mimotopes and putative heparin binding sequences obtained from phage specifically eluted from laminin-1 by peptide 11 or by heparan sulfate

Sequence homology with	Sequences from phage eluted by peptide 11 ^a	Sequences eluted by heparan sulfate ^a
LBP ²⁰⁵⁻²²⁹	RDPEEIEKEEQAAAEKAVTKEEFOG GMKAVR IQG GKAMLDRA SHATVKA AV	RDPEEIEK EEQAAAEKAVTKEEFOG DRTAMQVAA DRTAMQVAA VVSKESEAG GGSVAFRAG
LBP - Peptide G	IPCNNKGAHSVGLMWWMLAREVLRMR KPWWRTINA (6) WHRTMWWP (8) PWWMTTRHW ^c	IPCNNKGAHSVGLMWWMLAREVLRMR GPGAWWGS
LBP - C-terminal DWS containing repeats	QPATEDWS QN TD WLGNL (3)	QPATEDWS None
Putative heparin binding sequences ^d	HARSHYPWY KWKWPDRPK SLEHRAFRN GKLNLGKYK KMNKGVVNP	SKMHRNSWF AKIPAGRDR KMNKGVVNP

Number of multiple isolations are shown in parentheses.

^a Residues contributing to the homology are shown in bold and underlined.

^b Residues showing homology with the mimotopes are underlined.

^c Previous sequence in reverse order.

^d Positively charged residues in putative heparin binding peptides are shown in bold.

scrambled YIGSR sequence peptide has previously been shown to retain some, albeit much reduced, activity in other experiments (Yoshida *et al.*, 1999).

BLAST searches for similarities to phage LBP mimotope and putative heparin-binding sequences

BLAST searches were run against the OWL composite sequence database (218,197 sequences) for all of the phage insert sequences shown in Table 2 to look for sequence matches in other proteins. None of the phage LBP²⁰⁵⁻²²⁹ mimotope sequences eluted by peptide 11 were found in identical form in the database, and no more than three poor matches in other proteins were found for any of these sequences. No matches were found for one of the phage LBP²⁰⁵⁻²²⁹ mimotope sequences eluted by heparan sulfate. The other two yielded poor sequence matches in two and seven proteins respectively. Somewhat better matches were found for phage mimotopes of the LBP peptide G domain. Two modest and nine poor sequence matches were found for the WHRTMWWWP peptide eluted by peptide 11, and two modest and four poor sequence matches were found for the GPGAWWGS peptide eluted by heparan sulfate. Only four poor sequence matches were found for the QNTDWLGNL peptide, a mimotope for the LBP DWS containing repeats. No matches at all were found for two of the putative heparin binding sequences, and between two and nine poor sequence matches were obtained for the remaining six phage sequences. In all cases, the proteins in which the limited sequence matches were found were of very diverse functions. Overall, the very limited pattern of "match" sequences obtained in the BLAST searches confirm the likely specificity of the phage sequence mimotopes for the LBP sequence.

Phage clones carrying LBP mimotopes re-bind directly to laminin-1

In order to confirm the binding specificity of phage populations specifically eluted from laminin-1, we chose six such phage clones and compared their abilities to bind to laminin-1 with the wild type phage population in an ELISA plate assay. The phage clones from the specific elutions were chosen to represent phage carrying insert sequences mimicking each of the three regions for which LBP mimotopes were obtained (Table 2). As shown in Figure 1, all clones that were tested displayed significantly higher affinity for laminin-1 than the wild-type phage. These data suggest that all three regions of the LBP identified by the existence of mimotopes in the peptide library may play a role in binding to laminin-1, and that each of them may be independently capable of binding.

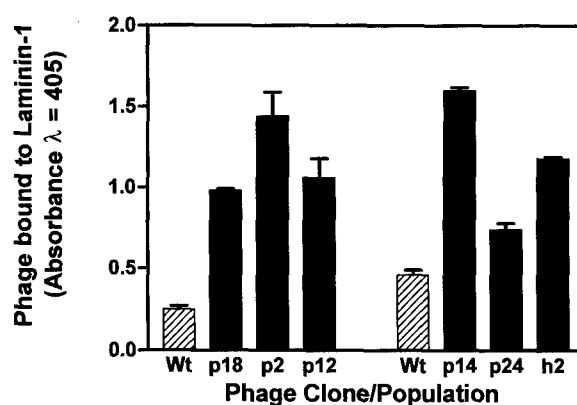


Figure 1. ELISA assays showing the ability of specifically eluted phage clones to bind to laminin-1. The assays were carried out as described in Materials and Methods, and the data shown is the average of replicate wells \pm SD. Wild-type M13 phage were used as a control. We tested two clones containing peptide G mimotopes (p18, KPWWRTNTA; p24, WHRTMWWWP), three clones containing mimotopes for LBP²⁰⁵⁻²²⁹ (p14, GKAMLDLRAS; p2, GMKAVRIQG and h2, DRTAMQVAA) and a clone with the mimotope for the DWS-containing C-terminal repeats (p12, QNTDWLGNL). Clones with a "p" designation were eluted with peptide 11 and the clone with an "h" designation was eluted with heparan sulfate.

Peptide 11 binds and crosslinks the LBP²⁰⁵⁻²²⁹ peptide in a dose-dependent manner

To further investigate the possibility that the LBP²⁰⁵⁻²²⁹ domain could bind directly to laminin-1 at the peptide 11 site, as has been implicated previously by us (Landowski *et al.*, 1995b), we examined the ability of a photoactivatable cross-linking analog of peptide 11 (Starkey *et al.*, 1999) to bind and crosslink synthetic LBP²⁰⁵⁻²²⁹ peptide in an ELISA assay, as described in Materials and Methods. In our previous studies (Starkey *et al.*, 1999), we demonstrated the exquisite specificity of the peptide 11-based photoprobe. Using a Western protocol, we showed that, of the very large number of proteins present in an NP-40 detergent extract of tumor cell membranes, only one was biotinylated by this reagent. The biotinylated protein was of the correct molecular weight for the LBP. Figure 2 shows the dose dependent crosslinking of the peptide 11 analog to the LBP²⁰⁵⁻²²⁹ peptide. We repeated this assay three times, and, in each case, maximal crosslinking was obtained close to the LBP²⁰⁵⁻²²⁹ peptide concentration shown in Figure 2, with crosslinking decreasing appreciably at higher concentrations. We have examined the LBP²⁰⁵⁻²²⁹ peptide using circular dichroism (CD) spectroscopy and two dimensional proton NMR spectroscopy. At modest concentrations, the peptide exhibits a CD spectrum consistent with predominantly alpha helical structure (data not shown). However, at the higher concentrations needed for NMR spec-

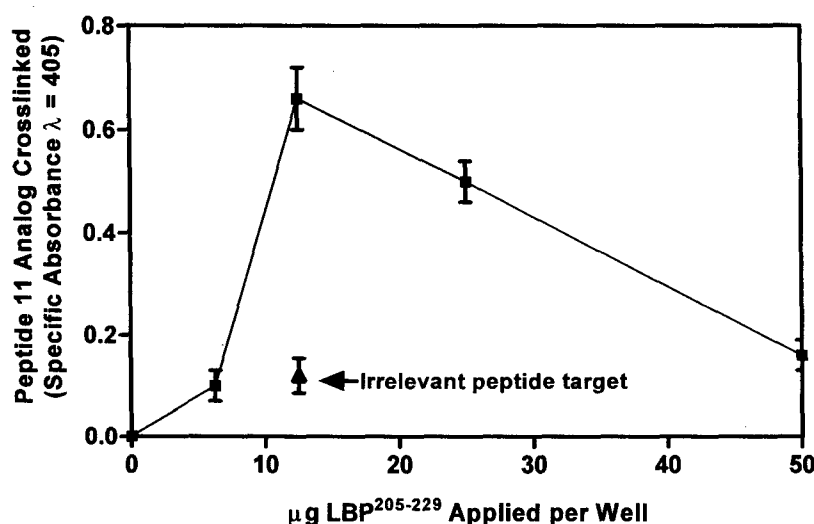


Figure 2. ELISA plate assay showing binding and crosslinking of the peptide 11 based photo-activatable analog to synthetic LBP²⁰⁵⁻²²⁹ peptide. Synthetic LBP²⁰⁵⁻²²⁹ peptide was allowed to bind to positively charged Primaria® plates as described in the Materials and Methods. The peptide 11 based photoprobe was added, and the plates UV irradiated as described in the Materials and Methods. Bound photoprobe was quantitated using avidin neutralite followed by biotinylated alkaline phosphatase and disodium p-nitrophenyl phosphate chromogenic substrate. Four replicates were used per dilution and the data shown is the average of the replicates \pm SD. The irrelevant pep-

tide target, included as a specificity control was the laminin-1 peptide, AFSTLEGRPSAY. The maximum specific absorbance obtained from wells coated with 12.5 μ g per well of the control peptide is shown.

troscopy, the NMR spectrum suggested significant aggregation of the peptide (data not shown). Such aggregation might be expected from the highly charged nature of the peptide, and it would also be expected to interfere with binding interactions to other ligands. We feel that the decrease in apparent ligand binding at higher LBP²⁰⁵⁻²²⁹ peptide concentrations in the ELISA assay is probably due to aggregation of the LBP²⁰⁵⁻²²⁹ peptide. Nevertheless, at favorable concentrations, the peptide 11 analog clearly bound and crosslinked to the LBP²⁰⁵⁻²²⁹ peptide in a dose dependent and reproducible manner.

Modeling of the LBP²⁰⁵⁻²²⁹ peptide sequence reveals potential heparin binding characteristics

Heparin binding protein domains are frequently helical with positive charges occurring close together on one side of the helix (Cardin & Weintraub, 1989; Deprez & Inestrosa, 1995). The LBP²⁰⁵⁻²²⁹ region is predicted to be mainly α -helical (Landowski *et al.*, 1995b), and a synthetic peptide with this sequence gives a strong α -helical signal by CD (data not shown). When a helical wheel plot of the relevant sequence was evaluated, we found that three positively charged Lys residues occurred on one side of the helix (Figure 3). Negatively charged Glu residues flank two of the Lys residues in the helical conformation (Figure 3). By examining the linear sequence and the helical wheel plot, we could not readily anticipate the likely relationship of the three positively charged Lys sidechains to each other, and to the sidechains of the negatively charged Glu residues. We, therefore, modeled the three-dimensional structure using the InsightII and Discover programs (MSI). After running a molecular dynamics experiment

and conducting energy minimization on the resultant structures, as described in Materials and Methods, we evaluated the final low energy structure as an example of a possible conformation for this domain of the 67 kDa LBP. Opposite sides of this potential structure are shown in Figure 4. Overall, the structure exhibited a helical backbone bent into a shallow comma shape (data not shown). Figure 4(a) shows the putative heparin/heparan sulfate-binding side of the helix. From this type of modeling, we were able to deduce that the sidechains of the three positively charged Lys residues discussed above are likely to project together in a longitudinal linear array down one face of the helix. Negatively charged sidechains flank this linear array. We concluded that this side of the helix probably could bind heparin or heparan sulfate. However, the closeness of the negatively charged residues would likely reduce the avidity of binding, and could provide for conformationally dependent binding. The other side of the helix (Figure 4(b)) shows a relative paucity of positively charged residue sidechains. Towards the C terminus, there exists a hydrophobic patch including a phenyl alanine sidechain. This hydrophobic patch is compatible with a docking site for peptide 11. It is known that the tyrosine residue in peptide 11 must be solvent exposed for bioactivity (Kawasaki *et al.*, 1994; Maeda *et al.*, 1994; Zhao *et al.*, 1994; Starkey *et al.*, 1998), and it is very likely that its sidechain docks to peptide 11 binding proteins (Starkey *et al.*, 1998).

Synthetic LBP²⁰⁵⁻²²⁹ peptide binds to isolated heparan sulfate

We utilized an ELISA plate assay to determine if isolated heparan sulfate could bind to synthetic LBP²⁰⁵⁻²²⁹. Increasing concentrations of isolated

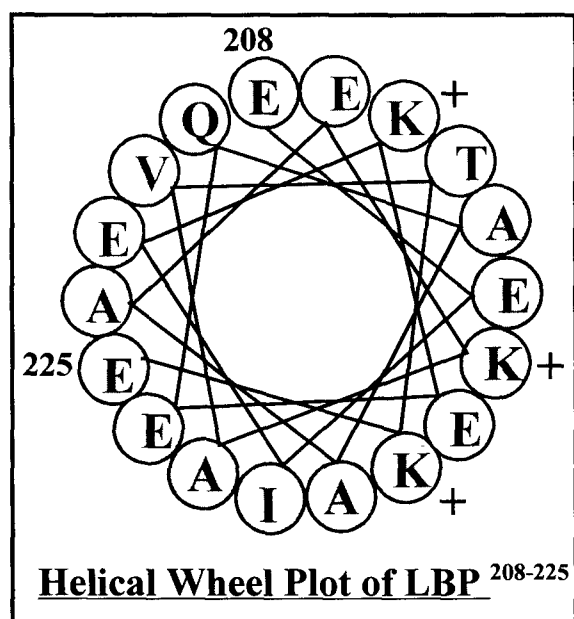


Figure 3. Helical wheel plot for LBP²⁰⁸⁻²²⁵. The start and end residues as well as the positively charged Lys residues are indicated by residue number or + as appropriate.

heparan sulfate were allowed to bind to positively charged Primaria[®] tissue culture 96-well plates as described in Materials and Methods. One hundred micrograms of synthetic LBP²⁰⁵⁻²²⁹ peptide was added per well, and the amount bound determined using our rabbit sequence specific antibody raised against this peptide (Landowski *et al.*, 1995a,b). An irrelevant peptide from the protein kinase C^{β1} sequence, H-C-(STYTANPEFVIANV-OH), and an antibody specific for this peptide were used to assess the potential for non-specific binding to heparan sulfate in the ELISA assay. Minimal binding to the target plate was observed for this peptide, and binding did not increase with increasing amounts of heparan sulfate. Specific binding of the LBP²⁰⁵⁻²²⁹ peptide to heparan sulfate was observed, and increased with increasing concentration of heparan sulfate to a plateau at 4 μg heparan sulfate per well (Figure 5). This experiment was repeated twice with similar results, and indicates that synthetic LBP²⁰⁵⁻²²⁹ peptide can bind isolated heparan sulfate as is predicted by the phage display experiments and modeling studies reported in this manuscript.

Synthetic QPATEDWSA peptide inhibits cell adhesion to laminin-1

In the course of sequencing of the recombinant inserts of the 38 phage specifically eluted by peptide 11 in round 6, we observed a sequence QNTDWLGNL in three individual isolates (Table 2). This peptide exhibits a sequence similarity to the TEDWS sequence which is repeated with minor variations five times within the most

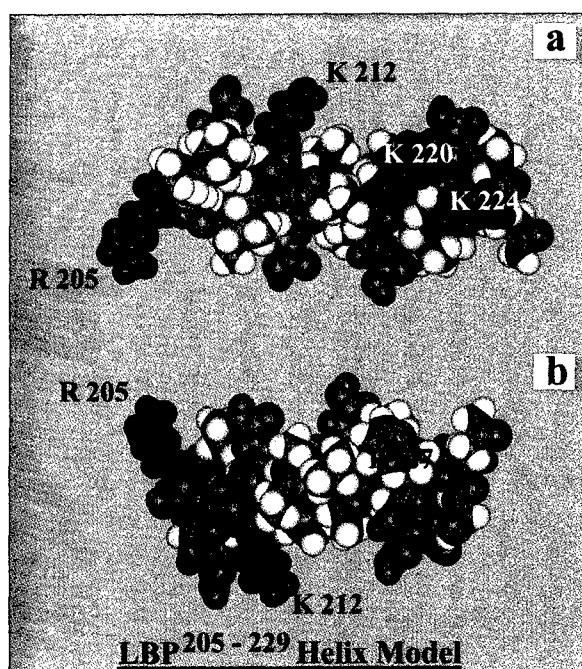


Figure 4. Computer based model of the LBP²⁰⁵⁻²²⁹ domain. The structure is shown after a molecular dynamics simulation and extensive energy minimization. (a) Putative heparin-binding side, and, (b) putative peptide 11 binding side. Residues with positively charged side-chains (blue) and residues with negatively charged side-chains (red).

C-terminal domain of the LBP. To determine the biological relevance of this sequence, we synthesized a peptide derived from the LBP with the sequence of the third repeat, QPATEDWSA, and tested its ability to interfere with cell adhesion to laminin-1.

Laminin-1 was coated on the wells of a 96 well tissue culture plate as described in Materials and Methods, and the QPATEDWSA peptide was used at a concentration of 100 μg/ml. Cell attachment was measured at several time points from 5 to 120 minutes after cell addition using the MTT (3-[4,5-dimethylthiazol-2-yl]-2,5-diphenyltetrazolium bromide) metabolite to quantitate adherent cells. Three tumor cell lines were assayed. B16BL6 mouse melanoma cells were used as a representative highly invasive and metastatic cell line, and DG44CHOwt and DG44CHOα6β1 as chinese hamster ovary cell variants exhibiting modest and high co-expression of the 67 kDa LBP and the α6β1 laminin-specific integrin (Starkey *et al.*, 1999). For B16BL6 cells, a clear inhibition of attachment was evident by ten minutes after addition of the cells in the presence of the synthetic peptide, and this became more intense by 15 minutes after addition of the cells (Figure 6). At later time points, the difference between peptide treated and control cells gradually diminished. A similar profile for inhibition of the rate of attachment was seen for DG44CHOwt cells in the presence of the

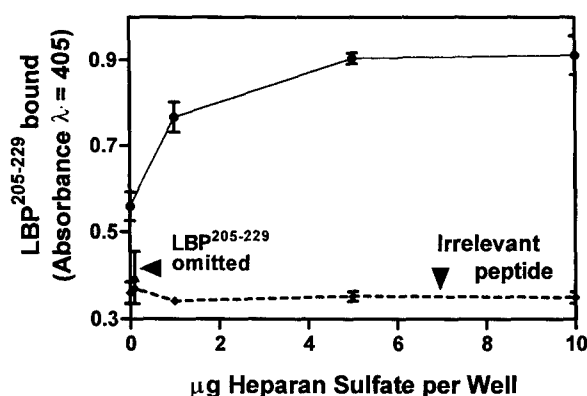


Figure 5. ELISA plate assay showing binding of synthetic LBP²⁰⁵⁻²²⁹ peptide to heparan sulfate bound to a positively charged Primaria[®] plate. Binding of the synthetic LBP²⁰⁵⁻²²⁹ peptide was quantitated using our LBP²⁰⁵⁻²²⁹ specific rabbit antibody, followed by alkaline phosphatase conjugated anti-rabbit IgG and the chromogenic p-nitrophenyl phosphate substrate. Each data point represents the average of six replicates \pm SEM.

QPATEDWSA peptide (Figure 6). The scrambled peptide, WAQADSTPE did not inhibit binding of DG44CHOwt cells to laminin-1 (Figure 6), supporting the importance of the QPATEDWSA sequence to bioactivity of the peptide. DG44CHO cells attach more slowly to laminin-1 than do B16BL6 cells. Therefore, the 30 minute time point for DG44CHO cells is roughly equivalent to the 15 minute time point which is shown for B16BL6 cells. The synthetic peptide had no apparent effect of the attachment of DG44CHO α 6 β 1 cells (Figure 6). Since these cells express much more 67 kDa LBP and α 6P1 integrin receptor than the DG44CHOwt cells (Starkey *et al.*, 1999), the simplest explanation for their lack of sensitivity to the effects of the QPATEDWSA peptide, is that the amount of peptide present was insufficient to affect the large number of laminin binding proteins expressed by these cells. These results support a direct interaction of the QPATEDWSA peptide with cellular laminin-1 binding proteins, but does not indicate whether the 67 kDa LBP or the α 6 β 1 integrin is involved.

Discussion

Screening of random sequence phage display peptide libraries is a powerful technique which allows for mapping of the regions on a protein surface which are involved in protein-protein interactions (DeLeo *et al.* 1995; van Zonneveld *et al.*, 1995; James *et al.*, 1997). Since it was first described in 1990 (Scott & Smith, 1990; Devlin *et al.*, 1990), it has rapidly become a tool of choice for investigators seeking to identify interfacial sequences between proteins (DeLeo *et al.*, 1995; James *et al.*, 1997) and for epitope mapping (Ryan *et al.*, 1998; Fack *et al.*, 1997; Henderikx *et al.*, 1998; Tarassishin *et al.*, 1999). Phage display experiments have been

used in a variety of systems, including mapping of protein-protein interactions involved in cell adhesion (O'Neil *et al.*, 1994; Koivunen *et al.*, 1994; Ryan *et al.*, 1998; Welply *et al.*, 1996; Healy *et al.*, 1995; Kraft *et al.*, 1999). Our preliminary data indicated that populations of phage eluted by peptide 11 immediately after the non-specific elution rounds expressed inserts which were dominated by sequences containing tryptophan residues, aromatic and positively charged residues. Heparan/heparin-binding motifs are often characterized by enrichment in basic amino acids juxtapositioned to tryptophan residues (Guo *et al.*, 1992a; Cardin & Weintraub, 1989), and it appeared likely that these sequences represented heparin-binding peptides. By employing serial specific elutions, consisting of heparan sulfate followed by peptide 11 elutions, we managed to eliminate a subpopulation of phage whose binding to laminin-1 is dependent on GAG. In this way, we largely overcame the predominance of putative heparin-binding phage recovered from elution with peptide 11. Putative heparin-binding phage dominated the early rounds of elution from laminin-1, to the extent that in the first round of specific selection 91% of the total eluted phage were recovered in the heparan sulfate fraction. Further selection with peptide 11 elution resulted in a significant reduction of phage in the heparan sulfate eluate. However, a heparan sulfate labile population persisted in the later rounds suggesting that peptide 11 itself could destabilize binding of this class of phage. Additional studies will be needed to ascertain if these particular phage clones bind to one or more sites on isolated laminin-1 and its residual associated GAG.

The majority of displayed peptide sequences from phage eluted with heparan sulfate in round six revealed multiple short stretches of linear homology with the R²⁰⁵-G²²⁹ region of the LBP. As indicated earlier, this region probably is of α -helical conformation. Therefore, we analyzed the sequences of these phage inserts both from the point of view of linear sequence homology, and for mimicking spatial epitopes formed by residues three or four apart in the primary sequence, a spacing which would place them adjacent in a helical fold. This analysis revealed additional sites of homology, mostly based on localization of charged residues (data not shown).

Of the sequenced inserts from the phage eluted by peptide 11 in round six, we found one insert, KPWWRTNA, with a homology to the palindromic sequence within LBP peptide G. We also found a number of sequences with homology to the R²⁰⁵-G²²⁹ region of LBP. Amongst these, some phage displayed linear sequence homology (Table 2), while others appeared to be mimicking the spatial distribution of charged residues on the surface of the presumed α helix structure of this region (data not shown). The sequence, QNTDWLGNL, was found in three independent isolates. This sequence is reminiscent of the DWS-containing repeats which are found in the C-terminal portion

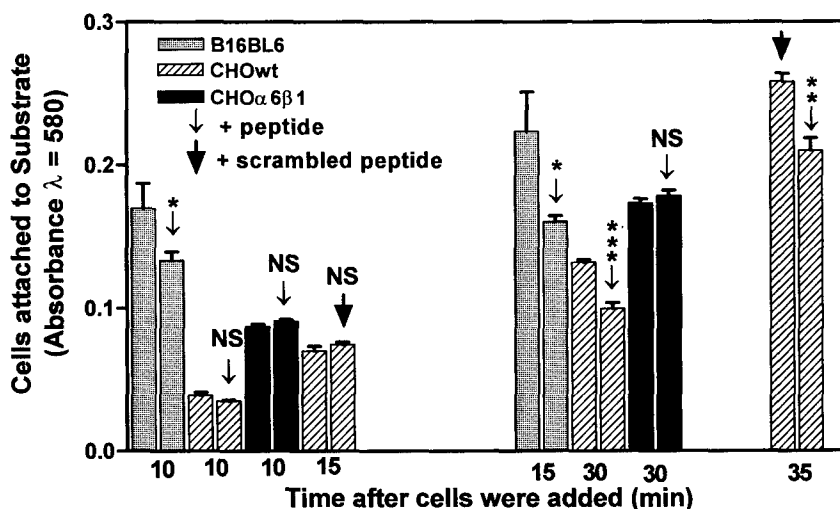


Figure 6. Cell adhesion assay to laminin-1 coated on a 96-well tissue culture plate as described in Materials and Methods. Data is shown for B16BL6 mouse melanoma cells and for two variants of the DG44CHO chinese hamster ovary cell line. The number of adherent cells was quantitated using the MTT assay, and data is shown for various time points in the presence and the absence of the QPATEDWSA synthetic peptide. The scrambled sequence peptide, WAQADSTPE, was used as a sequence specificity control. The data shown is the average of six replicate wells \pm SEM. Statistics were calculated using a *t*-test. **p* < 0.05, ***p* < 0.01 and ****p* < 0.001. NS = no statistical difference between data sets.

of the LBP. Although an antibody raised to a 20 residue long LBP peptide containing a single DWS repeat has been shown to disrupt cell binding to laminin-1 (Wewer *et al.*, 1987), no bioactivity had been ascribed to the repeat sequence itself. In the current report, we show that a peptide consisting of only this sequence does reduce the rate of cell binding to laminin-1 (Figure 6), so the repeat sequence is likely responsible for bioactivity of this region.

All residues involved in protein:protein interactions need not be mimicked by a single recombinant phage insert. The primary limitation is the size of the insert in the phage display peptide library that is utilized. It has been reported that some interacting surfaces simply cannot be adequately mapped using libraries with short (6 residues long) inserts, while libraries with longer (12-20 residues) inserts produce reliable mapping (Stephen *et al.*, 1995). In the current project, we used a library with 9-mer inserts, which carries some limitation on the size of epitope that can be mimicked by a single phage. We observed stretches of homology covering, at best, five continuous residues. Further, the sequences that we did obtain fell into the class of mimotopes. Amongst the phage that mimic the LBP²⁰⁵⁻²²⁹ region most homology is found with the region comprised by the K²²⁰ AVT²²³ residues. Interestingly, this same quadruplet is mimicked both by phage eluted by peptide 11 and by phage eluted by heparan sulfate. While heparan sulfate did elute some phage with putative heparin binding characteristics, none of these had any linear sequence homology with the LBP²⁰⁵⁻²²⁹. It is not clear why numerous sequences with homology to the

LBP²⁰⁵⁻²²⁹ were found in the heparan sulfate eluate from round six. It is possible that excess free heparan sulfate might interact with the heparin binding site in the proximal globular domain on the laminin β 1 chain, causing a structural change in the LE repeats where the peptide 11 sequence is located. Such a conformational change might result in release of phage bound to the LE repeat through LBP²⁰⁵⁻²²⁹-like sequences.

We obtained mimotopes for part of the LBP¹⁶¹⁻¹⁸⁰ region (peptide G). Interestingly, these mimotopes were seen in inserts from phage isolated from both peptide 11 and heparan sulfate eluates. As indicated earlier, we expected to see sequences with similarities to peptide G in the heparan sulfate eluates. Their presence in phage from the peptide 11 eluates was not expected, especially since peptide G was previously shown to interact with laminin-1 in a YIGSR - independent manner (Castronovo *et al.*, 1991b). One possible explanation for this apparent discrepancy with our phage display findings could result from effects which peptide G is suspected to have on the conformation of laminin-1 (Magnifico *et al.*, 1996). These conformational changes have been proposed to explain the fact that pre-treatment of laminin with peptide G in solution increases its binding to the cell surface, probably by exposing conditional receptor binding sites within laminin-1 (Magnifico *et al.*, 1996). Elution of LBP²⁰⁵⁻²²⁹-like sequences from the peptide 11-containing site on laminin-1 could cause conformational changes in the nearby heparan sulfate binding domain of the laminin β 1 chain. However, ligand photo-crosslinking and site-directed mutagenesis experiments will be needed to determine if one or more binding sites

in laminin-1 are involved in binding by the phage clones examined in the current study.

The phage display mapping reported in this manuscript strongly suggests that peptide 11 interacts with the LBP²⁰⁵⁻²²⁹ region. To test how these observations can be accommodated by the likely structure of this region, we performed computer simulated modeling experiments of this region. As shown in Figure 4(b) hydrophobic stretches ²¹⁶AAA²¹⁸ and ²²¹AVT²²³ contribute residues to a hydrophobic pocket on the surface of the α -helix. The aromatic F²²⁷ side-chain also faces into this pocket. On the N-terminal side, this pocket is flanked by K²¹², and on the C-terminal end by ²²⁵E. Peptide 11, CDPGYIGSR, contains a negatively charged residue in the second position and a C-terminal positively charged residue. Both charged residues are required for bioactivity (Starkey *et al.*, 1998) and may contribute to ligand binding. Therefore, it is possible that LBP residues K²¹² and E²²⁵ provide electrostatic attraction for peptide 11. The binding could be further stabilized by stacking of the aryl rings of peptide 11 Y⁵ and LBP F²²⁷. Our hypothesis that LBP²⁰⁵⁻²²⁹ is indeed a binding site for peptide 11 is supported by these simulations, and by the results of our ELISA experiment showing direct binding of the peptide 11 photo-cross-linking analog with the LBP²⁰⁵⁻²²⁹ peptide (Figure 2).

As indicated in the results section, the opposite side of the LBP²⁰⁵⁻²²⁹ helix demonstrates some features expected in a heparin-binding domain. A primary requirement for a "canonical" heparin binding site is significant enrichment in basic amino acid, and the binding domain is frequently helical in conformation (Cardin & Weintraub, 1989). The basic amino acid residues appear on the same side of the helix, forming a positively charged surface (Cardin & Weintraub, 1989). As shown in Figure 4(a), K²¹², K²²⁰ and K²²⁴ face the same side of the helix to form a linear array of positive charges. Therefore, this side of the LBP²⁰⁵⁻²²⁹ helix could, theoretically, bind heparin or heparan sulfate. Our ELISA assay confirmed that synthetic LBP²⁰⁵⁻²²⁹ could bind to immobilized heparan sulfate. From previous reports (Guo *et al.*, 1992b) we know that the binding of LBP to laminin *via* paptide G is mediated by heparan sulfate. Hence the presence of potential heparan sulfate binding domain on the "reverse" side of the LBP²⁰⁵⁻²²⁹ helix may also be biologically relevant.

Overall, the results presented in this manuscript indicate that binding of the 67 kDa LBP to laminin-1 is likely to be more complex than was previously thought. Heparan sulfate is probably an important alternative ligand, interacting not only with the peptide G sequence but also with LBP²⁰⁵⁻²²⁹. Based on the fact that peptide 11 can elute mimotopes of sequences found in the cDNA for the LBP, the peptide 11 sequence in laminin-1 would appear to be a binding site for the LBP. This has been questioned based on the results of rotary shadowing experiments where the dominant site for binding was

shown to be on the long arm of laminin-1 at a short distance from the peptide 11 site (Castronovo, 1993). In this earlier experiment, the fact that the LBP might exhibit binding to more than one site on this very large molecule was not fully considered. Indeed, the several heparin-binding sites present in laminin-1 make it likely that an isolated protein with heparin-binding characteristics would bind to multiple sites, albeit perhaps with different affinities. The most convincing argument for the importance of the peptide 11 sequence is the bioactivity of the synthetic peptide in inhibiting cellular activities dependent on interaction with laminin-1. If this sequence did not interact with the 67 kDa LBP, it would be necessary to postulate the involvement of another peptide 11 binding protein(s). Our own studies have shown that a photo-crosslinking peptide 11 analog only reacts with one detergent-extractable membrane protein with a mass appropriate for the 67 kDa LBP (Starkey *et al.*, 1999). However, although this finding and the evidence presented in the current manuscript strongly supports interaction of the 67 kDa LBP with the peptide 11-containing region of laminin-1, other approaches including additional analytical crosslinking experiments will need to be pursued to conclusively prove this.

Materials and Methods

Cell lines and tissue culture conditions

The highly invasive and metastatic murine melanoma cell line, B16BL6 (Post *et al.*, 1980), was obtained from the Mason Research Institute, Worcester, MA. The B16BL6 cells were propagated in RPM1 1640 medium (Sigma) supplemented with 10% fetal bovine serum (Gibco), 5 μ g/ml insulin and cover antibiotics. The DG44 variant of the CHO (Chinese hamster ovary) cell line was kindly provided by Dr L. Chasin of Columbia University. These cells are double mutants for the dihydrofolate reductase gene, and are used for methotrexate amplification of expression systems previously introduced along with a dhfr expression vector. Wild-type cells were propagated in α MEM medium (Sigma) containing 10% fetal bovine serum, hypoxanthine and thymidine, 5 μ g/ml insulin and cover antibiotics. Generation of the DG44CHO α 6 β 1 cells which overexpress the human α 6 and β 1 integrin chains is fully described by Starkey *et al.* (1999). Since these cells are methotrexate amplified for G418-selectable expression vectors, they are propagated in α MEM containing 60 μ M methotrexate and 400 μ g/ml G418 as well as 10% dialyzed fetal bovine serum, 5 μ g/ml insulin and cover antibiotics. Both the DG44CHO and the DG44CHO α 6 β 1 cell lines are highly invasive and metastatic in SCID mice.

The 9-mer random sequence phage display library

The J404 random sequence phage display library was generously donated by its creator, Dr Jim Burritt, Montana State University. The library was constructed by insertion of 27 bp synthetic oligonucleotides coding for random amino acids at the amino terminus of the minor phage coat protein III (Burritt *et al.* 1996). The chemical diversity of the library is estimated to be 5.7×10^8 . The

library was provided as primary unamplified stock. Unmodified M13 phage was used as the wild type in our experiments. J404 is expressed in the phage display vector, M13KBst, a filamentous M13 bacteriophage carrying a gene for kanamycin resistance. The bacteriophage was propagated in K91 *Escherichia coli* cells, and plaque assays were used to titrate the phage.

Reagents used in the biopanning and ELISA assays

Mouse EHS laminin-1 was purchased from Gibco Life Technologies (Grand Island, NY). Since all commercially available laminin-1 contains residual heparan sulfate bound to it (Guo *et al.*, 1992b), and, since it is far too expensive to remove it enzymatically, it is reasonable to assume that a small amount of heparan sulfate was present in all experiments, described in this manuscript, which utilized laminin-1. Bovine kidney heparan sulfate was purchased from Sigma Chemical Co. (St Louis, MO), and heparan sulfate from bovine lens capsule was isolated by us as described in (Robertson *et al.*, 1989). Peptide 11 (CDPGYIGSR) was synthesized at the Montana State University peptide synthesis facility on a Milligen 9050 automated peptide synthesizer using standard Fmoc chemistry with an amide carboxy terminus using PAL resin. The peptide was purified to homogeneity using a C18 reverse phase HPLC column (Vydac, Hesperia, CA), and the molecular weight verified using electrospray mass spectrometry. Peptide QPATEDWSA was purchased from Commonwealth Biotechnologies (Richmond, VA), and peptide LBP²⁰⁵⁻²²⁹ (RDPEEIEKEE-QAAAEKAVTKEEFQGG), laminin-1 peptide AFSTLE-GRPSAY, scrambled peptide 11 (SRYDGGICP) and scrambled QPATEDWSA (WAQADSTPE) were purchased from Macromolecular Resources (Fort Collins, CO). As described by Starkey *et al.* (1999), we synthesized an ultraviolet light photoactivatable crosslinker based on the peptide 11 sequence by replacing the tyrosine in the peptide 11 ligand with 4-benzoyl-L-phenylalanine. We also added a biotinylated lysine residue at the N terminus of the peptide, and included three glycine residues as a spacer between the biotinylated residue and the peptide 11 sequence to facilitate avidin binding. Bovine serum albumin (BSA, heat shock fraction IV) was purchased from Boehringer Mannheim (Indianapolis, MN). Glycine was purchased from Gibco Life Technologies, and Tris was purchased from Bio-Rad (Hercules, CA). All other chemicals were from Sigma Chemicals Co. (St Louis, MO). For biopanning, 60 mm Falcon[®] bacteriological Petri dishes (Becton Dickinson, Franklin Lakes, NJ) were used. Immulon[®] 2HB 96 well plates used for direct phage binding assay were from Dynex Technologies, Inc. (Chantilly, VA). Positively charged Primaria[®] and standard Falcon[®] tissue culture (Becton Dickinson, Franklin Lakes, NJ) microtiter plates were used for the direct peptide interaction ELISA assays as indicated elsewhere.

Screening of the phage display peptide library

Screening of the phage display peptide library for peptide inserts exhibiting binding affinity for laminin-1 was based on standard protocols described elsewhere (Smith & Scott, 1993). Two hundred micrograms of mouse laminin-1 in 2 ml of 0.1 M NaHCO₃ buffer was adsorbed to the surface of a 60 mm polystyrene Petri plate (Falcon[®]) during an incubation of ten hours at +4°C in a humidity chamber with constant agitation.

The plates were then blocked by incubation with 5 mg/ml dialyzed BSA (heat shock fraction IV, Boehringer Mannheim, MO) in 0.1 M NaHCO₃ buffer, before being washed seven times with 2 ml TTBS (Tris buffered saline containing 0.5% Tween-20). For the first round of selection, an aliquot of the phage display library representing 5×10^{12} phage was added to the plate. In consecutive rounds, aliquots of 30 to 50 μ l of amplified phage ($\sim 10^{10}$ PFU/ μ l) from the previous round were used. The aliquots of amplified phage were added in TTBS, and unbound phage were removed with seven washes of 2 ml TTBS. Bound phage were eluted using 0.1 M HCl-glycine, pH = 2.2, for five minutes with agitation. Eluted phage were immediately transferred to a fresh tube, and the solution was neutralized by addition of 1 M Tris. Eluted phage were amplified and re-panned on immobilized laminin-1. This procedure was repeated three times. In rounds 4, 5 and 6, we applied two consecutive specific elutions at neutral pH. These consisted of an elution with 700 μ g/ml mixture of heparan sulfates (50:50 (w/w)) from bovine kidney and bovine lens capsule in TBS, followed by an elution using 5 mM peptide 11 in TBS. The combined specific selection cycle was repeated two more times, to give a total of six rounds of phage selection and amplification. We tested a variety of inorganic buffers to achieve the maximal stringency of washing, and determined that Dulbecco's TPBS (phosphate buffered saline containing 0.5% Tween-20) was the most effective. Therefore, Dulbecco's TPBS was used for the washes in rounds 4, 5 and 6. Eluted phage were amplified in *E. coli* K-91, and titers of phage were monitored using a standard plaque forming assay. Phage elutions using an irrelevant laminin-1 bioactive peptide, AFSTLE-GRPSAY, and scrambled peptide 11, SRYDGGICP, were used to assess the specificity of peptide 11 eluted sequences.

ELISA assay for direct binding of phage to laminin-1

The wells of a 96-well Immulon 2HB plate were incubated with 100 μ l of a 25 μ g/ml laminin-1 in 0.1 M NaHCO₃ buffer for six hours at room temperature, followed by three hours of incubation at 37°C. The wells were then blocked by incubation with 150 μ l of 1% BSA in PBS for 12 hours. Phage stocks were titered immediately prior to use. Before adding these to the plate, the phage were diluted in PBS, and then 10^{10} , 10^9 and 10^8 PFU in 100 μ l were added per well. Phage were allowed to bind for ten hours at room temperature. Unbound phage were removed and the plates were washed six times in PBS/0.1% Tween-20. Rabbit anti-M13 antiserum was generously provided by Dr Algirdas Jesaitis, Montana State University. The IgG fraction was purified using immobilized protein A columns (Pierce, Rockford, IL), and was diluted in PBS/1% BSA. The working antibody dilution was determined empirically. One hundred microlitres of diluted anti-M13 antibody was loaded per well and allowed to react for four to six hours at room temperature. The plates were then rinsed as described above. Goat anti-rabbit IgG (H + L chain) alkaline phosphatase conjugated antibody (Bio-Rad) was diluted 1:1000 in PBS/1% BSA, and 100 μ l was loaded per well and allowed to react for four to six hours at room temperature. Then plates were again washed as described above. One hundred microliters enzyme substrate solution (0.5 mg/ml disodium *p*-nitrophenyl phosphate (Sigma) in 9.8% diethanolamine, 0.5 mM MgCl₂) was added per well, and absorbance readings at 405 nm were taken at several time points from five minutes to

two hours. The effectiveness of binding was determined by taking the ratio of the averages of absorbencies in replicate wells for the phage being tested and for wild-type phage in the 10^{10} PFU/well dilution. Specificity of binding was determined by comparing the "phage/wt" ratios for wells coated with laminin and wells without laminin.

BLAST searches using mimotope sequences

BLAST searches were run against the OWL composite database using settings suggested in the online/cited literature as appropriate for a short peptide query sequence. When matches were found, these were evaluated using the probability value assigned by the program. The poor sequence matches had probability values of 0.96 or larger, and the modest matches had probability values between 0.37 and 0.8. Although, it did not affect the ratings we gave these particular matches, we also checked the matching sequences for the presence of residues contributing to the classification of the query sequence as an LBP mimotope.

Direct binding and crosslinking of the photoactivatable peptide 11 analog to LBP²⁰⁵⁻²²⁹ peptide

Positively charged 96-well Primaria[®] plates were treated with 100 μ l of the LBP²⁰⁵⁻²²⁹ synthetic peptide per well at dilutions of 0.5 mg/ml, 0.25 mg/ml, 0.125 mg/ml and 0.0625 mg/ml in Dulbecco's phosphate buffered saline (PBS). Four replicates were used per dilution. The microwell plate was then incubated overnight at 4°C. After this, the peptide-containing solution was removed from the wells, 150 μ l of PBS containing 1% BSA was added to block the plate, and the plate was incubated at room temperature for a further two hours. The blocking solution was then removed, and the plate washed three times with PBS. For the assay, 80 μ l of the photoactivatable peptide 11 analog (Starkey *et al.*, 1999), freshly dissolved at a concentration of 0.167 mg/ml in PBS, was added per well. The plate was then subjected to a two minute irradiation with 350 nm long wave UV light (black light) as described by Starkey *et al.* (1999) to crosslink the peptide 11 analog to any binding sites. The analog-containing solution was then removed and the plate washed three times with PBS. One hundred microliters of a 1:1000 dilution of avidin neutralite (Molecular Probes, Eugene, OR) in PBS was then added to each well, and the plate was incubated at room temperature for one hour. After the avidin neutralite solution was removed, the plate was washed six times with PBS and 100 μ l of a 1:1000 dilution of biotinylated alkaline phosphatase (Bio-Rad) in PBS was added per well. The plate was then incubated for one hour at room temperature. Following removal of the biotinylated alkaline phosphatase and six washes with PBS, 100 μ l of p-nitrophenyl phosphate chromogenic substrate was added. The quantity of peptide 11 analog which bound and crosslinked to the LBP²⁰⁵⁻²²⁹ peptide was assessed using an ELISA plate reader measuring light absorption at 405 nm. Absorption from wells treated with BSA but no LBP²⁰⁵⁻²²⁹ peptide was subtracted from the final readings. Three individual assays were conducted, and each gave similar results. As a specificity control, the laminin-1 peptide, AFSTLEGRPSAY, was used as an irrelevant peptide target for crosslinking by the photoactivatable peptide 11 analog.

Heparan sulfate binding assay

Positively charged 96-well Primaria[®] microtiter plates were coated with heparan sulfate in increasing concentrations in PBS, pH = 7.0, and incubated for three hours at room temperature. The residual heparan sulfate solution was then removed, the wells were rinsed three times with PBS and blocked with 1% gelatin (Bio-Rad, ACS grade) in PBS for three hours at room temperature. The gelatin solution was then removed, wells washed seven times and 100 μ l of the LBP²⁰⁵⁻²²⁹ peptide in PBS (0.5 mg/ml) was loaded per well. The peptide was allowed to bind for 15 hours at room temperature. The wells were then washed multiple times with PBS, and binding of the peptide to heparan sulfate was detected using anti-LBP²⁰⁵⁻²²⁹ rabbit antibodies (Landowski *et al.*, 1995b) followed by alkaline phosphatase-conjugated goat anti-rabbit IgG (H + L chain) (Bio-Rad) (1:1000) in PBS. Chromogenic reaction with p-nitrophenyl phosphate was monitored by absorption at 405 nm. To assess the specificity of LBP²⁰⁵⁻²²⁹ peptide binding to heparan sulfate, an irrelevant peptide from the protein kinase C^{B1} sequence, H-C-(STYTANPEFVIANV-OH) (Calbiochem, San Diego, CA) was used in place of the LBP²⁰⁵⁻²²⁹ peptide in this assay. A rabbit antibody specific for this peptide (Calbiochem) was used in place of our rabbit anti-LBP²⁰⁵⁻²²⁹ antibody, and then the assay was developed as indicated above.

Cell adhesion inhibition assay

Ninety-six well microtiter plates (Falcon[®]) were coated with 100 μ l laminin-1 (50 μ g/ml in Dulbecco's PBS) and incubated for three hours at 37°C. The wells were then blocked by addition of 6% BSA solution to give a final concentration of 3% BSA, and were incubated for 15 hours at +4°C. The wells were briefly rinsed with Dulbecco' PBS immediately before use. Monodispersed suspensions of cells were obtained using minimal trypsin exposure. 10^4 cells were loaded per well in serum-free, protein-free medium with or without the QPATEDWSA peptide (100 μ g/ml) and were incubated in a tissue culture incubator at 37°C. After set time intervals, unattached cells were removed, the wells were washed twice with serum-free medium, and fresh medium was added. After the end of the adhesion period, medium in all wells was replaced with fresh medium containing MTT (0.25 mg/ml) and incubation was continued for three hours. The medium was then removed and the MTT metabolite was dissolved in DMSO. Absorbency readings were taken at 580 nm using a microtiter plate reader. Sequence specificity for bioactivity of the QPATEDWSA peptide was evaluated by substituting a peptide with scrambled sequence, WAQADSTPE, in the adhesion assay.

Computer-based modeling of a potential 3D structure for the LBP²⁰⁵⁻²²⁹ peptide

A model for the LBP²⁰⁵⁻²²⁹ region was built in an α -helical backbone conformation using the program, InsightII (MSI, Inc.). The initial structure was then energy minimized using the "steepest descents" then "conjugate gradients" algorithms in Discover (MSI, Inc.). Since the total energy of the structure was still relatively high and had not converged well, a molecular dynamics simulation was carried out using the Discover software package. The CVFF forcefield was employed for 200 ps of molecular dynamics with steps of 1 fs at 300 K.

Charges and cross terms were omitted from the potentials and harmonic bond stretching potentials were used. The lowest energy structure was then further energy minimized using "steepest descents" followed by "conjugate gradients" algorithms to give a final structure exhibiting a 40-fold reduction in total energy compared to the initial structure. This was considered to be a reasonable potential structure for the peptide.

Acknowledgments

This work was supported by NIH grant RO1 CA71561, and in parts by the US Army grant DAMD17-97-1-7207 and California BCRP grant 3CB-0183. We thank Edward A. Dratz, Deborah L. Berglund, Pati Glee, Seth Pincus, Tammy Schepp, Tami Peters and Jim Burritt for very helpful discussions.

References

- Ardini, E., Tagliabue, E., Magnifico, A., Butò, S., Castronovo, V., Colnaghi, M. I. & Ménard, S. (1997). Co-regulation and physical association of the 67 kDa monomeric laminin receptor and the $\alpha 6 \beta 4$ integrin. *J. Biol. Chem.* **272**, 2342-2345.
- Ardini, E., Pesole, G., Tagliabue, E., Magnifico, A., Castronovo, V., Sobel, M. E., Colnaghi, M. I. & Ménard, S. (1998). The 67-kDa laminin receptor originated from a ribosomal protein that acquired a dual function during evolution. *Mol. Biol. Evol.* **15**, 1017-1025.
- Burritt, J. B., Bond, C. E., Doss, K. W. & Jesaitis, A. J. (1996). Filamentous phage display of oligopeptide libraries. *Anal. Biochem.* **238**, 1-13.
- Butò, S., Tagliabue, E., Ardini, E., Magnifico, A., Ghirelli, C., Van den Brùle, F., Castronovo, V., Colnaghi, M. I., Sobel, M. E. & Ménard, S. (1998). Formation of the 67-kDa laminin receptor by acylation of the precursor. *J. Cell. Biochem.* **69**, 244-251.
- Cardin, A. D. & Weintraub, H. J. (1989). Molecular modeling of protein-glycosaminoglycan interactions. *Arteriosclerosis*, **9**, 21-32.
- Castronovo, V. (1993). Laminin receptors and laminin-binding proteins during tumor invasion and metastasis. *Invasion Metastasis*, **13**, 1-30.
- Castronovo, V., Claysmith, A. P., Barker, K. T., Cioce, V., Kruttsch, H. C. & Sobel, M. E. (1991a). Biosynthesis of the 67 kDa high affinity laminin receptor. *Biochem. Biophys. Res. Comm.* **177**, 177-183.
- Castronovo, V., Tarabozetti, G. & Sobel, M. E. (1991b). Functional domains of the 67-kDa laminin receptor precursor. *J. Biol. Chem.* **266**, 20440-20446.
- Colnaghi, M. I. (1994). The simultaneous expression of c-erbB-2 oncoprotein and laminin receptor on primary breast tumors has a predicting potential analogous to that of the lymph node status. *Adv. Exp. Med. Biol.* **353**, 149-154.
- Daidone, M. G., Silvestrini, R., Benini, E., Grigioni, W. F. & D'Errico, A. (1997). Expression of high-affinity 67-kDa laminin receptors in primary breast cancers and metachronous metastatic lesions or contralateral cancers. *British J. Cancer*, **76**, 52-53.
- De Manzoni, G., Guglielmi, A., Verlato, G., Tomezzoli, A., Pelosi, G., Schiavon, I. & Cordinano, C. (1998). Prognostic significance of 67-kDa laminin receptor expression in advanced gastric cancer. *Oncology*, **55**, 456-460.
- DeLeo, F. R., Yu, L., Burritt, J. B., Loetterle, L. R., Bond, C. W., Jesaitis, A. J. & Quinn, M. T. (1995). Mapping sites of interaction of p47-phox and flavocytochrome b with random-sequence peptide phage display libraries. *Proc. Natl Acad. Sci. USA*, **92**, 7110-7114.
- Deprez, P. N. & Inestrosa, N. C. (1995). Two heparin-binding domains are present on the collagenic tail of asymmetric acetylcholinesterase. *J. Biol. Chem.* **270**, 11043-11046.
- Devlin, J. J., Panganiban, L. C. & Devlin, P. E. (1990). Random peptide libraries: A source of specific protein binding molecules. *Science*, **249**, 404-406.
- Fack, F., Hugle-Dorr, B., Song, D., Queitsch, I., Petersen, G. & Bautz, E. K. (1997). Epitope mapping by phage display: random versus gene-fragment libraries. *J. Immunol. Methods*, **206**, 43-52.
- Ford, C. L., Randal-Whitis, L. & Ellis, S. R. (1999). Yeast proteins related to the p40/laminin receptor precursor are required for 20 S ribosomal RNA processing and the maturation of 40 S ribosomal subunits. *Cancer Res.* **59**, 704-710.
- Gasparini, G., Barbareschi, M., Boracchi, P., Bevilacqua, P., Verderio, P., Dalla-Palma, P. & Ménard, S. (1995). 67-kDa laminin-receptor expression adds prognostic information to intra-tumoral microvessel density in node-negative breast cancer. *Int. J. Cancer*, **60**, 604-610.
- Gho, Y. S., Lee, J. E., Oh, K. S., Bae, D. G. & Chae, C. B. (1997). Development of antiangiogenic peptide using a phage-displayed peptide library. *Cancer Res.* **57**, 3733-3740.
- Graf, J., Iwamoto, Y., Martin, G. R., Kleiman, H. K., Robey, F. A. & Yamada, Y. (1987a). Identification of an amino acid sequence in laminin mediating cell attachment, chemotaxis, and receptor binding. *Cell*, **48**, 989-996.
- Graf, J., Ogle, R. C., Robey, F. A., Sasaki, M., Martin, G. R., Yamada, Y. & Kleinman, H. K. (1987b). A pentapeptide from the laminin B1 chain mediates cell adhesion and binds the 67000 laminin receptor. *Biochemistry*, **26**, 6896-6900.
- Guo, N., Kruttsch, H. C., Negre, E., Vogel, T., Blake, D. A. & Roberts, D. D. (1992a). Heparin- and sulfatide-binding peptides from the type I repeats of human thrombospondin promote melanoma cell adhesion. *Proc. Natl Acad. Sci. USA*, **89**, 3040-3044.
- Guo, N., Kruttsch, H. C., Vogel, T. & Roberts, D. D. (1992b). Interactions of a laminin-binding peptide from a 33-kDa protein related to the 67-kDa laminin receptor with laminin and melanoma cells are heparin-dependent. *J. Biol. Chem.* **267**, 17743-17747.
- Halatsch, M.-E., Hirsch-Ernst, K. I., Kahl, G. F. & Weinel, R. J. (1997). Increased expression of $\alpha 6$ -integrin receptors and of mRNA encoding the putative 37 kDa laminin receptor precursor in pancreatic carcinoma. *Cancer Letters*, **118**, 7-11.
- Hall, H., Deutzmann, R., Timpl, R., Vaughan, L., Schmitz, B. & Schachner, M. (1997). HNK-1 carbohydrate-mediated cell adhesion to laminin-1 is different from heparin-mediated and sulfatide-mediated cell adhesion. *Eur. J. Biochem.* **246**, 233-242.
- Healy, J. M., Murayama, O., Maeda, T., Yoshino, K., Sekiguchi, K. & Kikuchi, M. (1995). Peptide ligands for integrin $\alpha v \beta 3$ selected from random phage display libraries. *Biochemistry*, **34**, 3948-3955.

- Henderikx, P., Kandilogiannaki, M., Petrarca, C., von Mensdorff-Pouilly, S., Hilgers, J. H. M., Krambovitis, E., Arends, J. W. & Hoogenboom, H. R. (1998). Human single-chain Fv antibodies to MUC1 core peptide selected from phage display libraries recognize unique epitopes and predominantly bind adenocarcinoma. *Cancer Res.* **58**, 4324-4332.
- Hung, M., Rosenthal, E., Boblett, B. & Benson, S. (1995). Characterization and localized expression of the laminin binding protein/p40 (LBP/p40) gene during sea urchin development. *Exp. Cell Res.* **221**, 221-230.
- Iwamoto, Y., Robey, F. A., Graf, J., Sasaki, M., Kleinman, H. K., Yamada, Y. & Martin, G. R. (1987). YIGSR, a synthetic laminin pentapeptide, inhibits experimental metastasis formation. *Science*, **238**, 1132-1134.
- Iwamoto, Y., Graf, J., Sasaki, M., Kleinman, H. K., Grotorex, D., Martin, G. R., Robey, F. A. & Yamada, Y. (1988). Synthetic pentapeptide from the B1 chain of laminin promotes B16F10 melanoma cell migration. *J. Cell. Phys.* **134**, 287-291.
- James, M., Man, N. T., Edwards, Y. H. & Morris, G. E. (1997). The molecular basis for cross-reaction of an anti-dystrophin antibody with alpha-actinin. *Biochim. Biophys. Acta*, **1360**, 169-176.
- Karpátová, M., Tagliabue, E., Castronovo, V., Magnifico, A., Ardini, E., Morelli, D., Belotti, D., Colnaghi, M. I. & Ménard, S. (1996). Shedding of the 67-kD laminin receptor by human cancer cells. *J. Cell. Biochem.* **60**, 226-234.
- Kawasaki, K., Murakami, T., Namikawa, M., Mizuta, T., Iwai, Y., Yamashiro, Y., Hama, T., Yamamoto, S. & Mayumi, T. (1994). Amino acids and peptides. XXI. Laminin-related peptide analogs including poly(ethylene glycol) hybrids and their inhibitory effect on experimental metastasis. *Chem. Pharm. Bull.* **42**, 917-921.
- Kleinman, H. K., McGarvey, M. L., Liotta, L. A., Robey, P. G., Tryggvason, K. & Martin, G. R. (1982). Isolation and characterization of type IV procollagen, laminin, and heparan sulfate proteoglycan from the EHS sarcoma. *Biochemistry*, **21**, 6188-6193.
- Kleinman, H. K., Weeks, B., Schnaper, H. W., Kibbey, M. C., Yamamura, K. & Grant, D. S. (1993). The laminins: A family of basement membrane glycoproteins important in cell differentiation and tumor metastases. *Vitamins Hormones*, **47**, 161-186.
- Koivunen, E., Wang, B. & Ruoslahti, E. (1994). Isolation of a highly specific ligand for the $\alpha_5\beta_1$ integrin from a phage display library. *J. Cell. Biol.* **124**, 373-380.
- Kraft, S., Diefenbach, B., Mehta, R., Jonczyk, A., Luckenbach, G. A. & Goodman, S. L. (1999). Definition of an unexpected ligand recognition motif for $\alpha_v\beta_6$ integrin. *J. Biol. Chem.* **274**, 1979-1985.
- Landowski, T. H., Dratz, E. A. & Starkey, J. R. (1995a). Studies of the structure of the metastasis associated 67 kDa laminin binding protein: fatty acid acylation and evidence supporting dimerization of the 32 kDa gene product to form the mature protein. *Biochemistry*, **34**, 11276-11287.
- Landowski, T. H., Selvanayagam, U. & Starkey, J. R. (1995b). Control pathways of the 67 kDa laminin binding protein: surface expression and activity of a new ligand binding domain. *Clin. Exp. Metastasis*, **13**, 357-372.
- Maeda, T., Titani, K. & Sekiguchi, K. (1994). Cell-adhesive activity and receptor-binding specificity of the laminin-derived YIGSR sequence grafted onto Staphylococcal protein A. *J. Biochem.* **115**, 182-189.
- Maeda, M., Izuno, Y., Kawasaki, K., Kaneda, Y., Mu, Y., Tsutsumi, Y., Nakagawa, S. & Mayumi, T. (1998a). Amino acids and peptides. XXXI. Preparation of analogs of the laminin-related peptide YIGSR and their inhibitory effect on experimental metastasis. *Chem. Pharm. Bull.* **46**, 347-350.
- Maeda, M., Kawasaki, K., Mu, Y., Kamada, H., Tsutsumi, Y., Smith, T. J. & Mayumi, T. (1998b). Amino acids and peptides - XXXIII. A bifunctional poly(ethylene glycol) hybrid of laminin-related peptides. *Biochem. Biophys. Res. Commun.* **248**, 485-489.
- Magnifico, A., Tagliabue, E., Butó, S., Ardini, E., Castronovo, V., Colnaghi, M. I. & Ménard, S. (1996). Peptide G, containing the binding site of the 67-kDa laminin receptor, increases and stabilizes laminin binding to cancer cells. *J. Biol. Chem.* **271**, 31179-31184.
- Massia, S. P., Rao, S. S. & Hubbell, J. A. (1993). Covalently immobilized laminin peptide tyr-ile-gly-ser-arg (YIGSR) supports cell spreading and co-localization of the 67-kilodalton laminin receptor with α -actinin and vinculin. *J. Biol. Chem.* **268**, 8053-8059.
- Ménard, S., Castronovo, V., Tagliabue, E. & Sobel, M. E. (1997). New insights into the metastasis-associated 67 kD laminin receptor. *J. Cell Biochem.* **67**, 155-165.
- Nomizu, M., Yamamura, K., Kleinman, H. K. & Yamada, Y. (1993). Multimeric forms of Tyr-Ile-Gly-Ser-Arg (YIGSR) peptide enhance the inhibition of tumor growth and metastasis. *Cancer Res.* **53**, 3459-3461.
- O'Neil, K. T., DeGrado, W. F., Mousa, S. A., Ramachandran, N. & Hoess, R. H. (1994). Identification of recognition sequences of adhesion molecules using phage display technology. *Methods Enzymol.* **245**, 370-386.
- Parthasarathy, N., Gotow, L. F., Bottoms, J. D., Kute, T. E., Wagner, W. D. & Mulloy, B. (1998). Oligosaccharide sequence of human breast cancer cell heparan sulfate with high affinity for laminin. *J. Biol. Chem.* **273**, 21111-21114.
- Pasqualini, R., Koivunen, E. & Ruoslahti, E. (1995). A peptide isolated from phage display libraries is a structural and functional mimic of an RGD-binding site on integrins. *J. Cell Biol.* **130**, 1189-1196.
- Pei, D. P., Han, Y., Narayan, D., Herz, D. & Ravikumar, T. S. (1996). Expression of 32-kDa laminin-binding protein mRNA in colon cancer tissues. *J. Surg. Res.* **61**, 120-126.
- Ponce, M. L., Nomizu, M., Delgado, M. C., Kuratomi, Y., Hoffman, M. P., Powell, S., Yamada, Y., Kleinman, H. K. & Malinda, K. M. (1999). Identification of endothelial cell binding sites on the laminin $\gamma 1$ chain. *Circ. Res.* **84**, 688-694.
- Poschl, E., Mayer, U., Stetefeld, J., Baumgartner, R., Holak, T. A., Huber, R. & Timpl, R. (1996). Site-directed mutagenesis and structural interpretation of the nidogen binding site of the laminin gamma chain. *EMBO J.* **15**, 5154-5159.
- Post, G., Doll, J., Hart, I. R. & Fidler, I. J. (1980). In vitro selection of murine B16 melanoma variants with enhanced tissue-invasive properties. *Cancer Res.* **77**, 1636-1640.
- Rao, C. N., Castronovo, V., Schmitt, M. C., Wewer, U. M., Claysmith, A. P., Liotta, L. A. & Sobel, M. E. (1989). Evidence for a precursor of the high-affinity

- metastasis-associated murine laminin receptor. *Biochemistry*, **28**, 7476-7486.
- Robertson, N. P., Starkey, J. R., Hamner, S. & Meadows, G. G. (1989). Tumor cell invasion of three-dimensional matrices of defined composition: evidence for a specific role for heparan sulfate in rodent cell lines. *Cancer Res.* **49**, 1816-1823.
- Romanov, V., Sobel, M. E., Pinto da Silva, P., Ménard, S. & Castronovo, V. (1994). Cell localization and redistribution of the 67 kD laminin receptor and $\alpha 6 \beta 1$ integrin subunits in response to laminin stimulation: an immunogold electron microscopy study. *Cell Adhes. Commun.* **2**, 201-209.
- Ryan, S. T., Chi-Rosso, G., Bonnycastle, L. L. C., Scott, J. K., Kotliansky, V., Pollard, S. & Gotwals, P. J. (1998). Epitope mapping of a function-blocking $\beta 1$ integrin antibody by phage display. *Cell Adhes. Commun.* **5**, 75-82.
- Sakamoto, N., Iwahana, M., Tanaka, N. G. & Osada, Y. (1991). Inhibition of angiogenesis and tumor growth by a synthetic laminin peptide, CDPGYIGSR-NH₂. *Cancer Res.* **51**, 903-906.
- Sanjuán, X., Fernández, P. L., Miquel, R., Muñoz, J., Castronovo, V., Ménard, S., Palacín, A., Cardesa, A. & Campo, E. (1996). Overexpression of the 67-kD laminin receptor. Correlates with tumour progression in human colorectal carcinoma. *J. Pathol.* **179**, 376-380.
- Satoh, K., Narumi, K., Isemura, M., Sakai, T., Abe, T., Matsushima, K., Okuda, K. & Motomiya, M. (1992). Increased expression of the 67 kDa-laminin receptor gene in human small cell lung cancer. *Biochem. Biophys. Res. Commun.* **182**, 746-752.
- Scott, J. K. & Smith, G. P. (1990). Searching for peptide ligands with an epitope library. *Science*, **249**, 386-390.
- Shaw, L. M. & Mercurio, A. M. (1994). Regulation of cellular interactions with laminin by integrin cytoplasmic domains: the A and B structural variants of the $\alpha 6 \beta 1$ integrin differentially modulate the adhesive strength, morphology, and migration of macrophages. *Mol. Biol. Cell*, **5**, 679-690.
- Smith, G. P. & Scott, J. K. (1993). Libraries of peptides and proteins displayed on filamentous phage. *Methods Enzymol.* **217**, 228-257.
- Starkey, J. R., Dai, S. & Dratz, E. A. (1998). Sidechain and backbone requirements for anti-invasive activity of laminin peptide 11. *Biochim. Biophys. Acta Protein Struct. Mol. Enzymol.* **1429**, 187-207.
- Starkey, J. R., Uthayakumar, S. & Berglund, D. L. (1999). Cell surface and substrate distribution of the 67-kDa laminin binding protein determined by using a ligand photoaffinity probe. *Cytometry*, **35**, 37-47.
- Stephen, C. W., Helminen, P. & Lane, D. P. (1995). Characterization of epitopes on human p53 using phage-displayed peptide libraries: Insights into antibody-peptide interactions. *J. Mol. Biol.* **248**, 58-78.
- Sung, U. (1997). Heparin binding of laminin: contribution of the triple helix in the rod domain to the formation of cryptic and active sites in the globular domain. *Mol. Cells*, **7**, 272-277.
- Tarassishin, L., Szawlowski, P., McLay, J., Kidd, A. H. & Russell, W. C. (1999). Adenovirus core protein VII displays a linear epitope conserved in a range of human adenoviruses. *J. Gen. Virol.* **80**, 47-50.
- Van den Brule, F. A., Berchuck, A., Bast, R. C., Liu, F. T., Gillet, C., Sobel, M. E. & Castronovo, V. (1994). Differential expression of the 67-kD laminin receptor and 31-kD human laminin-binding protein in human ovarian carcinomas. *Eur. J. Cancer*, **30A**, 1096-1099.
- van Zonneveld, A. J., van den Berg, B. M., van Meijer, M. & Pannekoek, H. (1995). Identification of functional interaction sites on proteins using bacteriophage-displayed random epitope libraries. *Gene*, **167**, 49-52.
- Viacava, P., Naccarato, A. G., Collecchi, P., Ménard, S., Castronovo, V. & Bevilacqua, G. (1997). The spectrum of 67-kD laminin receptor expression in breast carcinoma progression. *J. Pathol.* **182**, 36-44.
- Waltregny, D., De Leval, L., Ménard, S., De Leval, J. & Castronovo, V. (1997). Independent prognostic value of the 67-kd laminin receptor in human prostate cancer. *J. Natl Cancer Inst.* **89**, 1224-1227.
- Welply, J. K., Steininger, C. N., Caparon, M., Michener, M. L., Howard, S. C., Pegg, L. E., Meyer, D. M., De Ciechi, P. A., Devine, C. S. & Caspersen, G. F. (1996). A peptide isolated by phage display binds to ICAM-1 and inhibits binding to LFA-1. *Proteins: Struct. Funct. Genet.* **26**, 262-270.
- Wewer, U. M., Taraboletti, G., Sobel, M. E., Albrechtsen, R. & Liotta, L. A. (1987). Role of laminin receptor in tumor cell migration. *Cancer Res.* **47**, 5691-5698.
- Yoshida, N., Ishii, E., Yamada, Y., Mohri, S., Kinukawa, N., Matsuzaki, A., Oshima, K., Hara, T. & Miyazaki, S. (1999). The laminin-derived peptide YIGSR (Tyr-Ile-Gly-Ser-Arg) inhibits human pre-B leukaemic cell growth and dissemination to organs in SCID mice. *J. Cancer*, **80**, 1898-1904.
- Yow, H., Wong, J. M., Chen, H. S., Lee, C., Steele, G. D., Jr & Chen, L. B. (1988). Increased mRNA expression of a laminin-binding protein in human colon carcinoma: complete sequence of a full-length cDNA encoding the protein. *Proc. Natl Acad. Sci. USA*, **85**, 6394-6398.
- Zhao, M., Kleinman, H. K. & Mokotoff, M. (1994). Synthetic laminin-like peptides and pseudopeptides as potential antimetastatic agents. *J. Med. Chem.* **37**, 3383-3388.

Edited by M. Gottesman

(Received 15 December 1999; received in revised form 23 February 2000; accepted 8 March 2000)



DEPARTMENT OF THE ARMY
US ARMY MEDICAL RESEARCH AND MATERIEL COMMAND
504 SCOTT STREET
FORT DETRICK, MARYLAND 21702-5012

REPLY TO
ATTENTION OF:

MCMR-RMI-S (70-1y)

21 Feb 03

MEMORANDUM FOR Administrator, Defense Technical Information
Center (DTIC-OCA), 8725 John J. Kingman Road, Fort Belvoir,
VA 22060-6218

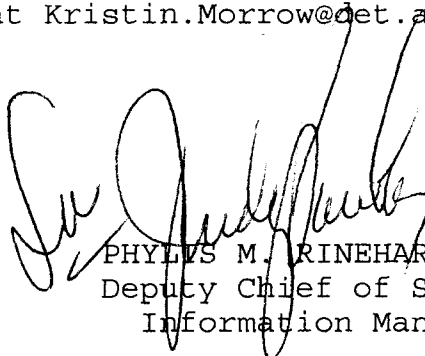
SUBJECT: Request Change in Distribution Statement

1. The U.S. Army Medical Research and Materiel Command has reexamined the need for the limitation assigned to technical reports written for this Command. Request the limited distribution statement for the enclosed accession numbers be changed to "Approved for public release; distribution unlimited." These reports should be released to the National Technical Information Service.

2. Point of contact for this request is Ms. Kristin Morrow at DSN 343-7327 or by e-mail at Kristin.Morrow@det.amedd.army.mil.

FOR THE COMMANDER:

Encl


PHYLLIS M. RINEHART
Deputy Chief of Staff for
Information Management

ADB263458	ADB282838
ADB282174	ADB233092
ADB270704	ADB263929
ADB282196	ADB282182
ADB264903	ADB257136
ADB268484	ADB282227
ADB282253	ADB282177
ADB282115	ADB263548
ADB263413	ADB246535
ADB269109	ADB282826
ADB282106	ADB282127
ADB262514	ADB271165
ADB282264	ADB282112
ADB256789	ADB255775
ADB251569	ADB265599
ADB258878	ADB282098
ADB282275	ADB232738
ADB270822	ADB243196
ADB282207	ADB257445
ADB257105	ADB267547
ADB281673	ADB277556
ADB254429	ADB239320
ADB282110	ADB253648
ADB262549	ADB282171
ADB268358	ADB233883
ADB257359	ADB257696
ADB265810	ADB232089
ADB282111	ADB240398
ADB273020	ADB261087
ADB282185	ADB249593
ADB266340	ADB264542
ADB262490	ADB282216
ADB266385	ADB261617
ADB282181	ADB269116
ADB262451	
ADB266306	
ADB260298	
ADB269253	
ADB282119	
ADB261755	
ADB257398	
ADB267683	
ADB282231	
ADB234475	
ADB247704	
ADB258112	
ADB267627	